Doctoral Thesis

Age-size structured models with stochastic growth and optimal life history
確率的成長下における齢—サイズ構造モデルと最適生活史

Graduate School of Environmental Science; Hokkaido University
ID 76085002

Ryo Oizumi

Contents

Preface

Stochastic analysis has been receiving much attention from researchers in many different fields, such as finance and statistical physics, and remarkable progress has been made. In particular, many mathematical tools, including Malliavin calculus, have been developed in stochastic differential equations and applied to these fields. Theoretical biologists formerly contributed to the development of stochastic analysis in population genetics, population ecology, and other fields. However, these applications of stochastic analysis to biology seem to have been no signifficant development over the last 30 years. Although stochasticity in the life history of organisms is recognized by empirical research, theorists still have applied deterministic models or used only computer simulations in studies of recent years. One reason for this is that stochastic analysis requires advanced knowledge of mathematics and fewer mathematical tools are available as compared to the situation in classic dynamic systems. Now, this situation is gradually changing.

In this study, we have produced innovations in several aspects of stochastic analysis. In Part I, we propose an age-size path-integral model induced by an age-size structured partial differential equation. The path-integral model

is not only a novel formularization of structured population models; it also provides a probability measure of stochastic size growth. This measure is used to provide all the expectations in this analysis. Part Ⅱ is devoted to an application of a Dirichlet boundary problem (the optimal stopping problem) to optimal life schedule problems in semelparous species and of stochastic control theory to life history. Part Ⅲ and Part Ⅳ provide analyses of specific examples of Part Ⅱ. This study should give as impetus to the systematization of theoretical biology in which we can analyze both deterministic and stochastic phenomena.

Part I
Introduction

Environmental change on a global scale is one of the world ' s great pending problems. Many ecologists are concerned that these changes will affect not only economic activity, but also the preservation of ecosystems and biodiversity. The effects of environmental change are considered to cause several stochasticities in ecosystems, including those in life histories. Ecological demographers have recently noted the effects of environmental stochasticity on population dynamics, including annual fluctuations in the total amounts of resources and climatic variations as well as demographic stochasticity [1]. Using transition matrix models (TMMs) [2, 3], ecologists have also shown another effect of stochasticity, which is the shortening of individual life spans. The most notable effect of stochasticity is considered to be the reduction of fitness [4, 5, 6]. Fitness is defined by the maximum eigenvalue in linear demographic models (LDMs), such as TMMs and integral projection models (IPMs), and reflects the population growth rate under a steady state of the population. Fitness in LDMs depends on elements of life history, e.g., body size and growth, survival, and stage transition rates. These vital rates

are affected by the life histories of each species. Therefore, environmental stochasticity should be considered when examining optimal schedule problems.

Generally, LDMs include two different kinds of stochasticities, namely, "internal stochasticity" and "external stochastisity." For example, in TMMs used by ecologists, internal stochasticity gives a species a set of transition probabilities to other states, whereas external stochasticity variegates the values of these transition probabilities annually. In other words, the former generates the transitions from a single state to multiple states, and the latter generates annual fluctuations in each element of the transition matrices. Then, the population vector at time t is in twofold stochasticity. Incidentally, demographers show that external stochasticity causes reductions in fitness by using a geometric mean of temporal fitness [7], whereby external stochasticity represents the environmental stochasticity for demographers and ecologists.

Corroborating whether twofold stochasticity yields annual fluctuations in finite populations is difficult because each individual does not always reflect all events generated by both stochasticities. Therefore, one may reasonably use an infinite dimensional population vector that can cover every event in the

environment. If the population vector includes only internal stochasticity, it satisfies a partial differential equation (PDE) [8], while if the population vector includes only external stochasticity, it satisfies a stochastic PDE (SPDE), as in [9], and is numerically analyzed by [10]. Most studies have examined the effects of external stochasticity on factors such as the population growth rate (fitness), life history traits, and life span [4, 5, 6, 2, 3, 9, 10]. However, few studies have noted the differences in the two stochasticities or have focused on the effects of internal stochasticity. Internal stochasticity has not attracted attention because, to date, we have not had the proper methods to analyze the effects of internal stochasticity. In brief, the effects of internal stochasticity on fitness are still far from well known.

In this study, we focus on internal stochasticity, which affects the body-size growth rate under r-selection. We construct a mathematical model of the stochastic life history of each individual using a stochastic differential equation (SDE) and analyze the relationship between optimal life history and population dynamics with stochasticity. Then, we hypothesize that the population vector is composed of continuous age and body size, and that the dynamics satisfy a PDE. We suggest that the solution of the PDE can

be expressed using path integrals. We will also show that the path-integral expression provides the IPM with a projection kernel. Consequently, our expression is consistent with other expressions of LDM. Additionally, we will derive the Euler–Lotka equation of stochastic growth, which connects fitness with life history. Then, we focus on an objective function generating the Euler–Lotka equation and several statistics of stochastic growth, such as the expectations of reproductive success and basic reproductive number, and the cumulant generating function of breeding age, derived from the function [11].

Furthermore, we introduce the ways in which optimal life schedule problems (OLSP) should be analyzed in r-selection with stochasticity. If internal stochasticity negatively affects fitness, the fittest individual is one possessing the optimal controls to avert the effects of stochasticity in the habitat. Accordingly, we focus on the control of internal stochasticity and use concepts of "Stochastic Control Theory" to build an optimal control for internal stochasticity. Then, we focus on applications of the objective function to analyze optimal stochastic growth strategies. First, we show the relationship between the age-size LDM and the Hamilton–Jacobi–Bellman (HJB) equation from control theory. Second, we apply this theory to analyze two

different breeding systems. Finally, we discuss the meaning of the maximized objective function and the relationship between the convexity of the function and optimal strategy.

Part II
Population vector with stochastic life history

In this section, we show a relationship between individual stochastic life history and population dynamics. We will construct a theory by the following procedure. First, we provide a general stochastic life history, which is composed of the stochastic growth rate of each individual, fertility rate, and survivorship functions including semelparity, iteroparity, and more general breeding systems. Second, we introduce the dynamics of a population vector following the above life history as an age-size structured model.

1 Assumptions of stochastic life history

We consider the growth rate of individuals with respect to body size $X_a \in A \subseteq \mathbb{R}_+$ at age a, A being the domain of body size. The growth rate is as follows:

$$\begin{cases} dX_a = g(X_a)\,da + \sigma(X_a)\,dB_a \\ \\ X_0 = x, \end{cases} \tag{1.1}$$

where x represents initial body size, and $g(0) = \sigma(0) = 0$. On the right-hand side, the first term is the drift, $g(X_a)$, which represents deterministic rule of

the size growth process; the second term, $\sigma(X_a)$, represents fluctuation at X_a, and B_a denotes Brownian motion. In addition, we assume Eq.(1.1) is Ito ' s SDE [12, 13] and set fertility and mortality functions, which depend on body size, y, as follows:

$$F(y) \geq 0, \tag{1.2}$$

$$\mu(y) > 0.$$

To consider a general life history, it is sufficient for fertility to have only integratablity here. Then, we define survivorship as follows:

$$S(a) := \exp\left\{-\int_0^a d\tau \mu(X_\tau)\right\}. \tag{1.3}$$

We here call Eqs.(1.1), (1.2), and (1.3) the set of life history equations.

2 Construction of the age-size structured model and offspring dynamics

Setting $P_t(a, y)$ as the population vector at time t and age a with growth from x to y, the dynamics of population vectors are well known to generally

follow a continuous age-size structured model:

$$\begin{cases} \left[\dfrac{\partial}{\partial t}+\dfrac{\partial}{\partial a}\right] P_t\left(a,y\right)=-\mathcal{H}_y P_t\left(a,y\right) \\ \mathcal{H}_y:=\dfrac{\partial}{\partial y}g\left(y\right)-\dfrac{1}{2}\dfrac{\partial^2}{\partial y^2}\sigma\left(y\right)^2+\mu\left(y\right) \\ P_{t-a}\left(0,y\right)=n_{t-a}\left(x\right)\delta\left(x-y\right), \end{cases} \tag{2.1}$$

where $\mathcal{H}_y$, $n_{t-a}\left(x\right)$, and $\delta\left(x-y\right)$ represent the Fokker–Planck Hamiltonian with mortality, initial number of offspring at time $t-a$, and Dirac delta, respectively, (see [14, 15]).

When we begin observations at time zero, the dynamics of offspring number $n_t\left(x\right)$ at time t follow the equation:

$$\begin{cases} n_t\left(x\right)=G_t\left(x\right)+\displaystyle\int_0^t da\int_A dyF\left(y\right)P_t\left(a,y\right) \\ G_t\left(x\right):=\displaystyle\int_t^\infty da\int_A dyF\left(y\right)P_t\left(a,y\right) \\ G_0\left(x\right)=n_0\left(x\right), \end{cases} \tag{2.2}$$

where $G_t\left(x\right)$ and $n_0\left(x\right)$ respectively represent a function, which gives a contribution of generations before the observation, and the initial number of offspring.

3 Path-integral expression of an age-size structured model

In this section, we introduce a new formalism of the population vector provided by a path-integral expression and provide a formal solution of Eq.(2.1). The functional form of the solution calculates the connection with a solution of classic age-structured models. Next, we show that the analysis of age-size transition can be equivalent to statistical physics approaches and to stochastic analysis in the path integral.

3.1 Introduction of a path-integral expression to the population vector

Using a path integral, we can decompose the solution of Eq.(2.1) into the initial population vector and projection function (Appendix A) as follows:

$$P_t(a, y) = n_{t-a}(x) K_a(x \to y). \tag{3.1}$$

Note that we set $K_0(x \to y) = \delta(x - y)$. $K_a(x \to y)$ represents the projection of growth from x to y at age a:

$$K_a(x \to y) := \lim_{\epsilon \to 0} \int_A \cdots \int_A \prod_{j=1}^{M-1} dx_j \prod_{j=0}^{M-1} K'_\epsilon(x_j \to x_{j+1}) \Big|_{M\epsilon=a, x_0=x, x_M=y},$$

where $K'_{\epsilon}(x_j \to x_{j+1})$ is projection at sufficiently short time ϵ and is expressed by

$$\begin{cases} K_a(x \to y) = \int_{X_0=x}^{X_a=y} \mathcal{D}(x) \int_{-\infty}^{\infty} \mathcal{D}(q) \exp\left\{ \int_0^a d\tau \left(-iq_\tau \dot{X}_\tau - \mathcal{H}(-iq_\tau, X_\tau) \right) \right\} \\ \mathcal{H}(-iq_\tau, X_\tau) := -iq_\tau g(X_\tau) + q_\tau^2 \sigma(X_\tau)^2 + \mu(X_\tau), \end{cases} \tag{3.2}$$

where q_τ represents an adjoint parameter, or

$$\begin{cases} K_a(x \to y) = \int_{X_0=x}^{X_a=y} \mathcal{D}(x) \exp\left\{ \int_0^a d\tau \mathcal{L}\left(\dot{X}_\tau, X_\tau \right) \right\} \\ \mathcal{L}\left(\dot{X}_\tau, X_\tau \right) := -\dfrac{\left(\dot{X}_\tau - g(X_\tau) \right)^2}{2\sigma(X_\tau)^2} - \mu(X_\tau). \end{cases} \tag{3.3}$$

$\mathcal{D}(\xi)$ denotes

$$\mathcal{D}(\xi) := \int \cdots \int \prod_{\tau \in (0,a)} d\xi_\tau,$$

(see Appendix A and E). The path integral is a summation over an infinity of possible growth curves connecting x with y with the sieve of mortality to compute the density in Eq.(1.3). Eqs.(3.2) and (3.3) are known in physics as the Hamiltonian expression and Lagrangian expression, respectively (the derivation is shown in Appendix A) [16]. The path integral is a limit of a Markovian process with respect to a short time interval ϵ keeping $M\epsilon = a$

and gives a specific expression of

$$\begin{aligned} P_t(a,y) &= n_{t-a}(x)\, K_a(x \to y) \\ &= n_{t-a}(x) \lim_{\epsilon \to 0} \int_A \cdots \int_A \prod_{j=1}^{M-1} dx_j \prod_{j=0}^{M-1} K'_\epsilon(x_j \to x_{j+1}) \Big|_{M\epsilon=a, x_0=x, x_M=y} \\ &= n_{t-a}(x) \lim_{\epsilon \to 0} \int_A \cdots \int_A \prod_{j=1}^{M-1} dx_j \prod_{j=0}^{M-1} p_\epsilon(x_j \to x_{j+1}) \\ &\quad \times \exp\left[-\epsilon \mu(x_j)\right] \Big|_{M\epsilon=a, x_0=x, x_M=y}, \end{aligned} \tag{3.4}$$

where $p_\epsilon(x_j \to x_{j+1})$ represents the transition probability of x_j to x_{j+1} and satisfies

$$K'_\epsilon(x_j \to x_{j+1}) = p_\epsilon(x_j \to x_{j+1}) \exp\left\{-\epsilon \mu(x_j)\right\}. \tag{3.5}$$

Therefore, the population vector of Eq.(3.1) also satisfies a solution of IPM [17, 18], such that

$$P_{t+\epsilon}(a+\epsilon, y) = \int_A d\xi K_\epsilon(\xi \to y)\, P_t(a, \xi). \tag{3.6}$$

It means that Eq.(3.6) is equivalent to Eq.(3.1). Then, $K_\epsilon(\xi \to y)$ plays a role of a projection kernel and satisfies

$$\int_A dy K_a(x \to y) = \mathbb{E}_x\left[S(a)\right]. \tag{3.7}$$

$\mathbb{E}_x\left[S(a)\right]$ represents the expectation of survivorship until age a starting from initial body size x. In justification of Eq.(3.7), the path integral provides

the specific probability measure of the stochastic growth and life history statistics, such as the basic reproductive number and mean life span, as defined by the measure.

The constitution of the projection function is important for understanding the population structure because all information on growth and survival is included in the function. Therefore, the projection function provides the age-size distribution with stochastic growth for each cohort, and its functional form is provided by a solution of the Fokker–Planck equation as follows:

$$\begin{cases} \dfrac{\partial}{\partial a} K_a\left(x \to y\right) = -\mathcal{H}_y K_a\left(x \to y\right) \\ \\ \quad K_0\left(x \to y\right) = \delta\left(x - y\right), \end{cases} \tag{3.8}$$

by substituting Eq.(3.1) into Eq.(2.1).

3.2 Connection of stochastic life history to statistical physics

An advantage of using a path-integral expression is that we can introduce a method popular in statistical physics, as in the following example, whereby a scale transformation is used in the path integral expression to obtain the Lagrangian solution. Eq.(1.1) generally has asymmetric noise generated by $\sigma\left(X_a\right)$. To clarify the effects of stochasticity on growth dynamics, we set

$\sigma(y) = \kappa\nu(y)$ $(\kappa > 0)$ in Eq.(1.1) and change the variable X_a to a new variable, Z_a [15], such that

$$Z_a = \int^{X_a} dy\nu(y)^{-1}, \tag{3.9}$$

and by using Ito's formula,

$$\begin{cases} dZ_a = \dfrac{d}{d\zeta}\mathcal{J}_\kappa(\zeta)\Big|_{\zeta=Z_a} da + \kappa dB_a \\ Z_0 = z \\ \mathcal{J}_\kappa(\zeta) := \displaystyle\int_z^\zeta dy \left[\frac{\bar{g}(y)}{\bar{\nu}(y)} - \frac{\kappa^2}{2}\frac{d}{dy}\bar{\nu}(y)\right] \end{cases} \tag{3.10}$$

where

$$\bar{g}(\zeta) := g \circ x^{-1}(\zeta), \bar{\nu}(\zeta) := \sigma \circ x^{-1}(\zeta),$$

is Smoluchowski equation [12, 13]) (x^{-1} represents the inverse function of Eq.(3.9)). Then, the new Hamiltonian in Eq.(2.1) becomes

$$\mathcal{H}_\zeta^\dagger = \frac{\partial}{\partial\zeta}\left(\frac{d}{d\zeta}\mathcal{J}_\kappa(\zeta)\right) - \frac{\kappa^2}{2}\frac{\partial^2}{\partial\zeta^2} + \bar{\mu}(\zeta), \tag{3.11}$$

where $\bar{\mu}(\zeta) = \mu \circ x^{-1}(\zeta)$. Using the function

$$r(\zeta) := \exp\left\{\frac{1}{\kappa^2}\mathcal{J}_\kappa(\zeta)\right\}$$

and the transform of $\mathcal{H}_{\zeta}^{\dagger}$, such that $\mathcal{O}_{\zeta} := r(\zeta)^{-1}\mathcal{H}_{\zeta}^{\dagger}r(\zeta)$, we obtain the following operator:

$$\begin{cases} \mathcal{O}_{\zeta} = -\dfrac{\kappa^2}{2}\dfrac{\partial^2}{\partial\zeta^2} + V(\zeta) \\ V(\zeta) := -\dfrac{1}{2\kappa^2}\left(\dfrac{d}{d\zeta}\mathcal{J}_{\kappa}(\zeta)\right)^2 + \dfrac{1}{2}\dfrac{d^2}{d\zeta^2}\mathcal{J}_{\kappa}(\zeta) + \bar{\mu}(\zeta). \end{cases} \tag{3.12}$$

Letting $K_a^{\dagger}(z \to \zeta)$ be a projection function of Eq.(3.10), it can now be expressed by a new projection function $W_a(z \to \zeta)$ as follows:

$$K_a^{\dagger}(z \to \zeta) = r(\zeta)\, W_a(z \to \zeta) \tag{3.13}$$

which is the solution of

$$\begin{cases} \dfrac{\partial}{\partial a}W_a(z \to \zeta) = -\mathcal{O}_{\zeta}W_a(z \to \zeta) \\ W_0(z \to \zeta) = r(\zeta)\,\delta(z-\zeta). \end{cases} \tag{3.14}$$

Then, the Lagrangian expression of Eq.(3.14) becomes the well-known path integral used in physics:

$$W_a(z \to \zeta) = \int_{Z_0=z}^{Z_a=\zeta} \mathcal{D}(z) \exp\left\{\int_0^a d\tau \left[-\frac{1}{2\kappa^2}\dot{Z}_a^2 - V(Z_a)\right]\right\}, \tag{3.15}$$

composed of infinitely many convolutions of the following Gaussian kernels

$$p_{\epsilon}(z_j \to z_{j+1}) = \frac{1}{\sqrt{2\pi\kappa^2\epsilon}} \exp\left\{-\frac{(z_{j+1}-z_j)^2}{2\kappa^2\epsilon}\right\}$$

obtained from Eq.(3.4), known as the Wiener measure [19]. Aside from the biological point of view, the dynamics of the rescaled body size Z_a behave like

Brownian motion in the potential field $V(\zeta)$. From Eqs.(3.13) and (3.15), we obtain

$$K_a^{\dagger}(z \to \zeta) = \int_{Z_0=z}^{Z_a=\zeta} \mathcal{D}(z) \exp\left\{ \int_0^a d\tau \mathcal{L}^{\dagger}\left(\dot{Z}_\tau, Z_\tau\right) \right\}$$
$$\mathcal{L}^{\dagger}\left(\dot{Z}_\tau, Z_\tau\right) := -\frac{1}{2\kappa^2}\left(\dot{Z}_\tau - \frac{d}{d\zeta}\mathcal{J}_\kappa(\zeta)\Big|_{\zeta=Z_\tau}\right)^2 - \frac{1}{2}\frac{d^2}{d\zeta^2}\mathcal{J}_\kappa(\zeta)\Big|_{\zeta=Z_\tau} - \bar{\mu}(Z_\tau). \tag{3.16}$$

Then, it is shown that a kinetic equation,

$$\dot{Z}_\tau = \frac{d}{d\zeta}\mathcal{J}_\kappa(\zeta)\Big|_{\zeta=Z_\tau}, \tag{3.17}$$

characterizes the size transition of the cohort. Let a body size, y_1, and the transformation, ζ_1, be an observed body size. If the trajectory of Eq.(3.17) reaches ζ_1 for all z, all individuals can reach the body size y_1 without accidental death with probability 1 [20]. We can analyze stochastic effects on the growth of individuals in the same way as the analysis of the deterministic dynamic system in Eq.(3.17).

Additionally, the path-integral expression tells us that mortality has the same meaning as potential energy in the theory of potential fields. From the Principle of Least Action, a classic growth curve reaching ζ at age a is expressed by inverse transformation of the solution in the Euler–Lagrange

equation:

$$\begin{cases} \left[\dfrac{d}{d\tau}\dfrac{\partial}{\partial \dot{Z}_\tau} - \dfrac{\partial}{\partial Z_\tau}\right]\mathcal{L}^\dagger\left(\dot{Z}_\tau, Z_\tau\right) = 0 \\ Z_0 = z, \qquad Z_a = \zeta. \end{cases} \tag{3.18}$$

We can obtain the growth curve of the original variable X_a directly by using the original Lagrangian (in Eq.(3.3)) and its Euler–Lagrange equation. Since both of the Lagrangians depend on mortality, the body-size transition curve is affected by mortality. In deterministic growth ($\kappa \to 0$), however, the dominant term of $\tilde{\mathcal{L}}$ becomes

$$\lim_{\kappa\to 0}\mathcal{L}^\dagger\left(\dot{Z}_\tau, Z_\tau\right) = -\frac{1}{2\kappa^2}\left(\dot{Z}_\tau - \frac{\bar{g}\left(Z_\tau\right)}{\bar{\nu}\left(Z_\tau\right)}\right)^2$$

and the effect of mortality on the size transition disappears, because all individuals have the same body size in each cohort. Therefore, it is a property of internal stochasticity that the body-size transition of cohorts does not match with individual growth, if mortality depends on body size.

Using the Wiener measure in Eq.(3.16), Brownian motion appears in the expectation of survivorship, Eq.(3.7), and can be rewritten as

$$\mathbb{E}_x\left[S\left(a\right)\right] = \mathbb{E}_z\left[\exp\left\{-\int_0^a d\tau V\left(B_\tau\right)\right\}\exp\left\{\frac{1}{\kappa^2}\mathcal{J}_\kappa\left(B_a\right) - \frac{1}{\kappa^2}\mathcal{J}_\kappa\left(z\right)\right\}\right]. \tag{3.19}$$

Eq.(3.16) shows that stochastic growth with size-dependent mortality is equivalent to a generalized random walk in the potential field, as explained in

[21, 22, 23]. The relationship between the path integral and life history of interest is beyond the scope of this study. We only emphasize that the solution of Eq.(2.1) can be decomposed into the initial population and the projection function by the path integral. Therefore, the path integral and Eq.(3.1) provide another formulation of LDM.

4 Euler–Lotka equation in stochastic life history

In this section, we derive the most important equation of this study from Eq.(2.2), as another powerful advantage of the path-integral formulation. The equation corresponds with the definition of the Euler–Lotka equation, which means a transformation from the life history to population growth rate. The analysis of the equation provides the optimal life schedule problem with an evolutional meaning. First, we derive a renewal equation of offspring dynamics from Eq.(3.1) by the method used by Feller [24]. Then, we calculate a new quantity, the expectation of reproductive success, in the renewal equation. Second, we can obtain the intrinsic rate of natural increase (here called fitness) by a well-known method. In the process of deriving fitness, we obtain an Euler–Lotka equation. However, this equation is different from the

classic Euler–Lotka because it is defined by the expectation of reproductive success.

4.1 Renewal equation in the age-size structured model

Substituting Eqs.(3.1) and (3.7) into Eq.(2.2)(see Eq.(3.4)), we obtain

$$\begin{aligned} n_t(x) =& G_t(x) + \int_0^t da \int_A dy F(y) P_t(a,y) \\ =& G_t(x) + \int_0^t da\, n_{t-a}(x)\, \mathbb{E}_x\left[F(X_a) S(a)\right], \end{aligned}$$

Additionally, we set a new function

$$u_a(x) := \mathbb{E}_x\left[F(X_a) S(a)\right] \tag{4.1}$$

denoting the expectation of reproductive success (ERS) at age a and obtain a renewal equation as follows:

$$\begin{cases} n_t(x) = G_t(x) + \int_0^t da\, n_{t-a}(x)\, u_a(x) \\ G_0(x) = n_0(x). \end{cases} \tag{4.2}$$

4.2 Euler–Lotka equation in internal stochasticity

The population growth rate is equal to the increasing rate of the number of offspring caused by the contribution before time zero and of reproductive success in each generation. The solution of Eq.(4.2) is derived from a well-

known method, as in Feller's work [24]. Setting a Laplace transformation of $G_t(x)$ and $u_a(x)$ in Eq.(4.2) as follows:

$$\begin{aligned}\hat{G}_\lambda(x) &:= \int_0^\infty dt \exp\{-\lambda t\} G_t(x) \\ \psi_\lambda(x) &:= \int_0^\infty da \exp\{-\lambda a\} u_a(x),\end{aligned} \tag{4.3}$$

the number of offspring becomes

$$n_t(x) = \lim_{\beta\to\infty} \frac{1}{2\pi i} \int_{\alpha-i\beta}^{\alpha+i\beta} d\lambda \exp\{\lambda t\} \frac{\hat{G}_\lambda(x)}{1-\psi_\lambda(x)}, \tag{4.4}$$

by using the inverse transform. Then, we name Eq.(4.3) "objective function." $n_t(x)$ can be rewritten by a dominant residue of RHS in Eq.(4.4), such that

$$n_t(x) = Q_x \exp\{\lambda^* t\} (1 + O(\exp\{-\eta t\})), \tag{4.5}$$

(known as the Sharp–Lotka–Feller theorem), where $Q_x, \eta > 0$ [25]. Then, λ^* is given by a dominant characteristic root of

$$1 = \psi_\lambda(x) = \int_0^\infty da \exp\{-\lambda a\} \mathbb{E}_x[F(X_a) S(a)]. \tag{4.6}$$

Additionally, the dominant root is always a real number because $u_a(x)$ is a bounded and positive function, and $\psi_\lambda(x)$ is a monotonic decreasing function with respect to λ. The dominant root is the intrinsic rate of natural increase.

Since Eq.(4.6) meets the definition of the Euler–Lotka equation [26], we refer to it as a Euler–Lotka equation in stochastic life history. The main difference from the classic Euler–Lotka equation is that the objective function is composed of ERS. Hereafter, we refer to the intrinsic rate of natural increase as ‘ fitness. ’

From Eqs.(3.1) and (4.5), we can write the general population vector with stochastic growth as follows:

$$P_t(a,y) = Q_x \exp\{\lambda^*(t-a)\}(1+O(\exp\{-\eta(t-a)\}))K_a(x\to y). \quad (4.7)$$

Thus, path-integral formulation provides the solution of Eq.(2.1) in an identical way to the McKendrick equation and gives a new objective function defined by ERS. From an evolutionary point of view, the optimal life schedule ought to maximize fitness in r-selection. To analyze the optimal life schedule, we require a function relating to the magnitude of fitness. That is, the key to analyzing the schedule problem is in λ^*, $u_a(x)$, and $\psi_\lambda(x)$.

5 Objective function and analysis

Thus far, the effects of life history on fitness have been shown to be obtainable by analyzing only the objective function. This section shows that $\psi_\lambda(x)$ has

an important role in analyzing general life history and demonstrates how we can obtain life history statistics from this function

First, we show how to derive the objective function using a stochastic analysis method. Second, we calculate the properties of life history, such as ERS, basic reproductive number, mean generation time, and mature age structure.

From the Feynman–Kac formula (Appendix B), the dynamics of ERS $u_a(x)$ satisfies

$$\begin{cases} \dfrac{\partial}{\partial a} u_a(x) = -\bar{\mathcal{H}}_x u_a(x) \\ \bar{\mathcal{H}}_x := -g(x)\dfrac{\partial}{\partial x} - \dfrac{1}{2}\sigma(x)^2 \dfrac{\partial^2}{\partial x^2} + \mu(x) \\ u_0(x) = F(x), \end{cases} \tag{5.1}$$

where $\bar{\mathcal{H}}_x$ is the formal adjoint operator of the Fokker–Planck Hamiltonian in Eqs.(2.1) and (3.2). Using the Laplace transform from Eq.(5.1), we obtain that the objective function $\psi_\lambda(x)$ satisfies the following:

$$-\left(\bar{\mathcal{H}}_x + \lambda\right)\psi_\lambda(x) + F(x) = 0. \tag{5.2}$$

Therefore, we can calculate the objective function as the solution of Eq.(5.2). In addition, this equation shows that the objective function depends on all the elements of life history. Accordingly, we introduce several characteristics

of life history, written using the function. For example,

$$\psi_0(x) = \int_0^\infty da u_a(x) \tag{5.3}$$

represents an expectation of the number of offspring over a lifetime and corresponds with a definition of basic reproduction number (BRN), or R_0 in mathematical demography [27]. Additionally, using the inverse transform of Eq.(4.3), we can obtain ERS without solving Eq.(5.1). Moreover, we show in the next section that life history statistics can be derived from the objective function and BRN.

Since internal stochasticity is generated by the dispersion of individual growth rates, breeding age represents the age at which organisms reproduce and becomes a useful statistic regardless of the breeding system of the organism. Letting $\Theta_\lambda(x)$ be a cumulant generating function of breeding age $a^\diamond$, it is simply expressed by expanding the logarithm of objective function into a Taylor series as follows:

$$\begin{aligned}\Theta_\lambda(x) &:= \log \psi_\lambda(x) \\ &= \sum_{l=0}^{\infty} \frac{(-\lambda)^l}{l!} \langle a^\diamond \rangle_x^{(l)}, \end{aligned} \tag{5.4}$$

and

$$\langle a^{\diamond}\rangle_{x}^{(l)} := \lim_{\lambda\to 0}\left[(-1)^{l}\frac{\partial^{l}}{\partial\lambda^{l}}\Theta_{\lambda,}\left(x\right)\right]. \tag{5.5}$$

For example, the expectation and variance of $a^{\diamond}$ are the cumulants of $l=1$ and $l=2$, respectively. Then, the density of $a^{\diamond}$ is given by the following function

$$\mathbb{A}\left(a\right) := \lim_{\beta\to\infty}\frac{1}{2\pi i}\int_{\alpha-i\beta}^{\alpha+i\beta} d\lambda \exp\left\{\lambda a\right\}\frac{\psi_{\lambda}\left(x\right)}{\psi_{0}\left(x\right)} = \frac{u_{a}\left(x\right)}{\psi_{0}\left(x\right)}. \tag{5.6}$$

The density function represents a breeding age distribution. Consequently, analyzing the objective function can provide us with useful information about characteristics of the breeding system and the population growth in internal stochasticity. In other words, the objective function represents the essence of a species in the framework of the analysis of this study. The effect of life schedule on fitness depends on how we choose the reproductive strategy in $F\left(y\right)$.

6 Application to semelparous species

In this section, we consider an effect of internal stochasticity on a semelparous life history because semelparous species reproduce only once during their lifetime. Thus, a species has to choose its reproductive timing in stochasticity.

Applying the general theory of this section to a semelparous life history, we show several statistics of a semelparous life schedule in this section.

6.1 Definition of a semelparous life schedule

In semelparous species, we denote mature body size $x^* > x$ and mature age a^*, such that

$$X_{a^*} = x^* \qquad a^* := \inf_a \{a > 0 | X_a \geq x^*\}, \tag{6.1}$$

fertility, $F_{\mathcal{S}}(y)$, is defined by

$$F_{\mathcal{S}}(y) := \delta_{y,x^*} \phi(y), \tag{6.2}$$

where δ_{y,x^*} represents Kronecker's delta; the fertility rate function $\phi(y)$ is a monotonically increasing function and satisfies $\phi(x^*) \geq 1$ at a mature body size x^*. Then, the mature age a^* is defined as the age at which a mature body size is attained. In semelparous species, mature age corresponds with breeding age ($a^\diamond = a^*$). Before attaining a mature age, individuals are affected by survivorship $S(a)$, which is identical to Eq.(1.3), and no individuals can survive past the mature age. Then, semelparous survivorship, $S_{\mathcal{S}}(a)$, becomes

$$S_{\mathcal{S}}(a) := \mathbf{1}_{\{a \in [0, a^*]\}} S(a). \tag{6.3}$$

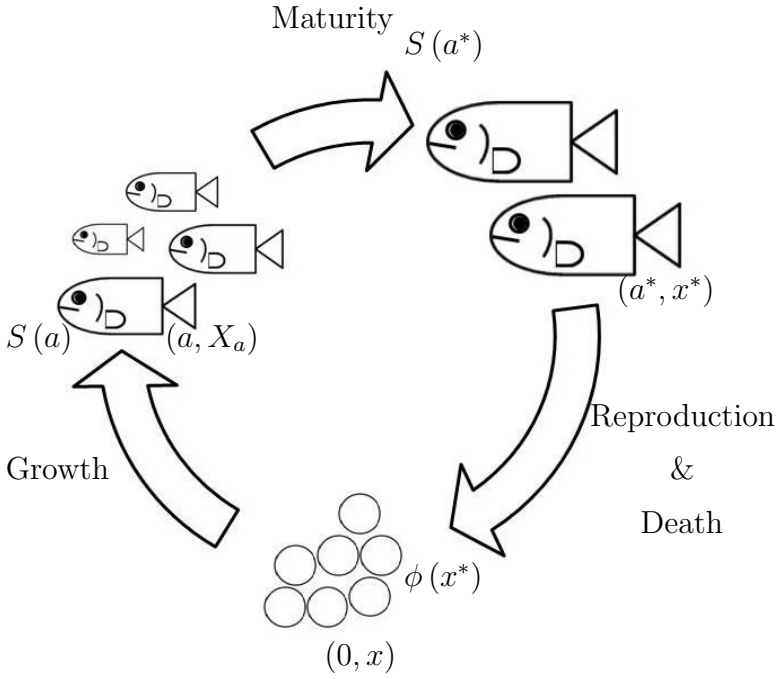

Figure 1: Life history of semelparous species with stochasticity. Each individual has the same initial body size x at age zero and grows at the rate of Eq.(1.1) with survivorship $S_{\mathcal{S}}(a)$ in Eq.(6.3) before attaining maturity (a^*, x^*). Then, mature individuals reproduce at the fertility rate function, $\phi(x^*)$.

Briefly stated, semelparous species grow at the rate of Eq.(1.1) with survivorship Eq.(6.3). Subsequently, the mature body size is attained x^*, and individuals reproduce at the rate of Eq.(6.2)(see Fig. 1). However, cohort dynamics are a simple formalization by path integrals because it is enough to choose the domain of body size A to $(0, x^*)$. Therefore, semelparous species

follow a conditional projection function, such that

$$K_a\left(x \to y \middle| y < x^*\right), \tag{6.4}$$

with the same Hamiltonian and Lagrangian as in Eqs.(3.2) and (3.3), respectively. The projection function represents a summation over every growth curve except when never reaching mature body size at age a and represents the solution of a boundary condition problem

$$K_a\left(x \to 0 \middle| y < x^*\right) = K_a\left(x \to x^* \middle| y < x^*\right) = 0 \tag{6.5}$$

in Eq.(3.8). Then, the projection function illustrates the size structure of juveniles in the cohort.

6.2 Objective function and statistics in semelparous life history

Since X_a has a strong Markov property from a property of Ito's SDE [12](see Appendix B), we can show the following relationship from Eq.(4.3):

$$\begin{aligned}\psi_{\mathcal{S}_{\lambda,x^*}}(x) &= \int_0^\infty da \exp\{-\lambda a\} u_a(x) \\ &= \mathbb{E}_x\left[\exp\{-\lambda a^*\} S_{\mathcal{S}}(a^*)\right] \phi(x^*).\end{aligned} \tag{6.6}$$

Additionally, we obtain a semelparous BRN written as

$$\psi_{\mathcal{S}_{0,x^*}}(x) = \mathbb{E}_x\left[S_{\mathcal{S}}(a^*)\right]\phi(x^*), \tag{6.7}$$

Eq.(5.4) becomes the cumulant generating function of mature age in semelparous species because semelparous breeding age is equivalent to mature age, $a^\diamond = a^*$. From Eq.(5.6), the probability density becomes the mature age density.

Part III
Stochastic control theory in life history

In this part, we focus on applications of the objective function to analyze optimal stochastic growth strategies. We show the relationship between the age-size LDM and the HJB equation from control theory and apply this theory to analyze two different breeding systems.

7 Configuration of life history and life schedule

To consider the optimal control of life history, in this section, we define life history with a control vector, as in section 1, and with details of semelparous and iteroparous life histories.

7.1 Body-size growth processes

We consider the growth rate of individuals with respect to a body size $X_a \in A \subseteq \mathbb{R}_+$ at age a, A being the domain of body size. The growth rate is as follows:

$$\begin{cases} dX_a = g\left(X_a, v\right) da + \sigma\left(X_a, v\right) dB_a \\ \\ X_0 = x, \end{cases} \tag{7.1}$$

where x represents initial body size, and $g(0,v) = \sigma(0,v) = 0$. On the right-hand side, the significance of $g(X_a, v)$, $\sigma(X_a, v)$, and B_a are identical to those of the RHS in Eq.(1.1). We set

$$v := (v_1, v_2, \cdots, v_d) \in \mathcal{V} \subset \mathbb{R}^d$$

to represent a control vector, with $\mathcal{V}$ as a compact convex set in $\mathbb{R}$. In addition, we assume that Eq.(7.1) is Ito's SDE [12, 13].

7.2 Fertility function and breeding systems

Semelparous and iteroparous breeding systems are defined as types of fertility function. In semelparous species, we use the fertility $F_{\mathcal{S}}(y)$, which is identical to Eq.(6.2), and we define an iteroparous fertility function $F_{\mathcal{I}}(y)$ as a continuous, second-order differentiable function, such that

$$F_{\mathcal{I}}(y) \geq 0, F_{\mathcal{I}}(y) \in C^2(A). \tag{7.2}$$

Then, the species can reproduce at any time during its growth stage.

We use fertility, Eq.(1.2), as a general breeding system if the analysis is common to semelparous and iteroparous breeding systems.

7.3 Mortality and survivorship

Semelparous and iteroparous species have different survivorships. We set a common mortality function depending on the body size y as follows:

$$\mu(y, v) > 0,$$

for both types of species. General survivorship $S(a)$ until age a is written as

$$S(a) = \exp\left\{-\int_0^a d\tau \mu(X_\tau, v)\right\}. \tag{7.3}$$

Since semelparous species die upon reproduction, we can set survivorship as

$$S_{\mathcal{S}}(a) := \mathbf{1}_{\{a\in[0,a^*]\}} S(a), \tag{7.4}$$

by using an indicator function and the general survivorship, Eq.(7.3). We assume that iteroparous species have a limit of their life span. Letting $\alpha \leq \infty$ be the limit of the life span, iteroparous survivorship is written as

$$S_{\mathcal{I}}(a) := \mathbf{1}_{\{a\in[0,\alpha)\}} S(a) \tag{7.5}$$

If the maximum life span follows $\alpha = \infty$, the species only dies by accidental death and Eq.(7.5) corresponds to Eq.(7.3).

7.4 Differences in life history between semelparity and iteroparity

In this section, we refer to Eq.(7.1), Eq.(1.2), and Eq.(7.3) as life history. Then, we define a semelparous and an iteroparous life history following Eqs.(6.2) and (7.4), and Eqs.(7.2) and (7.5) under the growth rate Eq.(7.1), respectively. In other words, we identify each life history by the differences in fertility and survivorship.

7.5 Population dynamics and objective function

This section gives a definition of the optimal schedule of reproductive timing and control of size growth under the life history parameters defined in the previous section. The population vector has Hamiltonian and Lagrangian expressions in the projection function, $K_a^v(x \to y)$, as follows:

$$\begin{cases} K_a^v(x \to y) = \int_{X_0=x}^{X_a=y} \mathcal{D}(x) \int_{-\infty}^{\infty} \mathcal{D}(q) \exp\left\{ \int_0^a d\tau \left(-iq_\tau \dot{X}_\tau - \mathcal{H}^v(-iq_\tau, X_\tau) \right) \right\} \\ \mathcal{H}^v(-iq_\tau, X_\tau) := -iq_\tau g(X_\tau, v) + q_\tau^2 \sigma(X_\tau, v)^2 + \mu(X_\tau, v), \end{cases} \tag{7.6}$$

and

$$\begin{cases} K_a^v(x \to y) = \int_{X_0=x}^{X_a=y} \mathcal{D}(x) \exp\left\{ \int_0^a d\tau \mathcal{L}^v\left(\dot{X}_\tau, X_\tau \right) \right\} \\ \mathcal{L}^v\left(\dot{X}_\tau, X_\tau \right) := -\dfrac{\left(\dot{X}_\tau - g(X_\tau, v) \right)^2}{2\sigma(X_\tau, v)^2} - \mu(X_\tau, v), \end{cases} \tag{7.7}$$

respectively. Then, fitness is provided by the dominant characteristic root of

$$\psi_{\lambda}^{v}(x) = 1, \tag{7.8}$$

where

$$\psi_{\lambda}^{v}(x) := \int_{0}^{\infty} da \exp\{-\lambda a\} \mathbb{E}_{x}^{v}\left[F(X_a) S(a)\right], \tag{7.9}$$

(see Eq.(4.6)). Eq.(7.8) is an Euler–Lotka equation in stochastic growth. The integral equation in offspring dynamics is identical to Eq.(2.2)

$\psi_{\lambda}^{v}(x)$ represents the Laplace transform of ERS and satisfies the theorem proved by Taylor *et. al* (1974) and Leon (1976) because the function is monotonically decreasing in λ [28, 29]. The theorem shows that a strategy maximizing $\psi_{\lambda}^{v}(x)$ is equivalent to maximizing fitness. Therefore, we can adopt $\psi_{\lambda}^{v}(x)$ as an objective function in the optimal life schedule with stochastic growth. Hereafter, we call $\psi_{\lambda}^{v}(x)$ the "objective function." Then, we extend the theorem to analyze the optimal life history with internal stochasticity (Appendix C).

8 Optimal life history

In 1970_s, a basic optimal strategy theorem was proven by Taylor *et.al* and Leon in a general deterministic environment [28, 29] and the theorem shows

that an optimal strategy, maximizing fitness, is equivalent to maximizing the following function,

$$\int_0^\infty da \exp\{-\lambda a\} F_a S_a,$$

where F_a and S_a represent the fertility rate and survivorship at age a. This function has identical significance to the objective function in this study and generates an Euler–Lotka equation in deterministic structured models [25]. The key point of the proof is that the objective function is a monotonically decreasing function in λ. Since this objective function clearly satisfies the condition, we extend the theorem to this life history model as follows:

Theorem

Let x^*_{opt} *be*

$$x^*_{opt} \in A, \quad \text{s.t.} \quad \lambda^*_{x^*_{opt},x} = \sup_{x^*} \lambda^*_{x^*,x},$$

and $\psi_{\lambda,x^*}(x)$ *is given by Eq.*(6.6). *Define* λ^*_{opt} *by*

$$\lambda^*_{opt} := \lambda_{x^*_{opt},x}.$$

Then, we have

$$\psi_{\lambda^*_{opt},x^*}(x) \leq \psi_{\lambda^*_{opt},x_{opt}}(x) \Leftrightarrow \lambda^*_{x^*,x} \leq \lambda^*_{x^*_{opt},x}.$$

This theorem can be proved identical to the proof of Appendix C. Now, we

show that the theorem holds for stochasticity by using an example, and that $\psi_\lambda(x)$ corresponds with the function used in the next section.

The optimal schedule problem considers the way in which a species chooses its reproductive timing to maximize its fitness with stochastic growth. We can prove the optimal theorem, as in Taylor *et.al* and Leon's works (see Appendix C) [28, 29]. Since the mature age (a^*) is defined by mature size (cf. Eq.(6.1)), finding the optimal mature age is equivalent to finding the mature size that maximizes the objective function. The approach is known as the optimal stopping problem in probability theory [12]. Then, we introduce three symbols: the optimal size x^*_{opt}, age $\tilde{a}$, and fitness λ^*_{opt}.

9 HJB equations and analysis

From the optimal life schedule theorem, the optimal life history strategy is equivalent to finding the function $\tilde{\psi}_\lambda(x)$, defined as

$$\tilde{\psi}_\lambda(x) := \sup_{v\in\mathcal{V}} \int_0^\infty da \exp\{-\lambda a\} \mathbb{E}^v_x \left[F(X_a) S(a)\right], \tag{9.1}$$

from Eq.(7.9). This function is known as a "value function" in control theory. The value function is the solution of the following equation:

$$\begin{cases} -\inf\limits_{v\in\mathcal{V}} \left\{\bar{\mathcal{H}}^v_x + \lambda\right\} \tilde{\psi}_\lambda(x) + F(x) = 0 \\ \bar{\mathcal{H}}^v_x := -g(x,v)\dfrac{d}{dx} - \dfrac{1}{2}\sigma(x,v)^2 \dfrac{d^2}{dx^2} + \mu(y,v). \end{cases} \tag{9.2}$$

Then, $\bar{\mathcal{H}}_x^v$ represents the formal adjoint operator of $\mathcal{H}_y^v$ in Eq.(7.6). Eq.(9.2) is the HJB equation used in the analysis of optimal controls [30, 12]. Since Eq.(9.2) is nonlinear and the solution generally does not have sufficient smoothness, the value function is interpreted as a "viscosity solution" in Eq.(9.2) (Appendix D). The derivation of Eq.(9.2) is shown in Appendix C. When Eq.(9.2) has a unique solution in the viscosity sense, we can obtain an optimal control $v_\lambda^*(x)$, such that

$$\psi_\lambda^{v^*}(x) = \tilde{\psi}_\lambda(x) \tag{9.3}$$

from the theorem on p.228 in [12]. Note that the optimal control v^* is a function of λ and has a degree of freedom. To derive the fitness of a species having optimal control, we substitute Eq.(9.1) into Eq.(7.8) and obtain the fitness, $\tilde{\lambda}$. Then, we have a unique optimal control:

$$\tilde{v}(x) := v_\lambda^*(x)\Big|_{\lambda=\tilde{\lambda}}. \tag{9.4}$$

Moreover, the optimal growth process becomes

$$\begin{cases} d\tilde{X}_a = g\left(\tilde{X}_a, \tilde{v}\left(\tilde{X}_a\right)\right) da + \sigma\left(\tilde{X}_a, \tilde{v}\left(\tilde{X}_a\right)\right) dB_a \\ \tilde{X}_0 = x, \end{cases} \tag{9.5}$$

from Eq.(7.1). An optimal control depending on only body size is known as a Markovian control. In the next subsection, we discuss the differences

in optimal growth processes between semelparous and iteroparous species. Value functions for each type of species are characterized by different HJB equations.

9.1 Optimal growth process and HJB equations in semelparous species

Due to the strong Markov property of the SDE, Eq.(7.1), the objective function of semelparous species, $\psi_{\mathcal{S}^v_{\lambda,x^*}}(x)$, can be generally written as

$$\begin{aligned}\psi_{\mathcal{S}^v_{\lambda,x^*}}(x) &= \int_0^\infty da \exp\{-\lambda a\} \mathbb{E}_x\left[F_{\mathcal{S}}(X_a) S_{\mathcal{S}}(a)\right] \\ &= \mathbb{E}^v_x\left[\exp\{-\lambda a^*\} S(a^*)\right] \phi(x^*), \end{aligned} \tag{9.6}$$

(Appendix B). Then, semelparous species have two optimal life schedule problems: (1) how to determine the optimal mature body size and (2) how to control the growth rate until that size is reached. The former is known as the "Optimal stopping problem" in probability theory, as mentioned in the previous subsection. To simplify the latter problem, we assume in this subsection that the mature body size exists. Setting the optimal mature age, $\tilde{a}$, and mature body size, x_{opt} ($:= X_{\tilde{a}}$), a value function of semelparity

becomes

$$\tilde{\psi}_{\mathcal{S}\lambda}(x) := \sup_{v\in\mathcal{V}} \sup_{x^*} \psi^{v}_{\mathcal{S}_{\lambda,x^*}}(x) = \sup_{v\in\mathcal{V}} \mathbb{E}^{v}_{x}\left[\exp\left\{-\lambda\tilde{a}\right\} S(\tilde{a})\right] \phi(x_{opt}). \tag{9.7}$$

This equation suggests that the optimal control optimizes the expectation of survivorship until the mature age, $\tilde{a}$. In other words, the evolution of a semelparous life history implies the optimization of life span.

Substituting Eqs.(6.2) and (7.4) into Eq.(9.2), the value function satisfies the boundary value problem of the following HJB equation:

$$-\inf_{v\in\mathcal{V}} \left\{\bar{\mathcal{H}}^{v}_{x} + \lambda\right\} \tilde{\psi}_{\mathcal{S}\lambda}(x) + F_{\mathcal{S}}(x) = 0. \tag{9.8}$$

From the semelparous fertility function, Eq.(6.2), the boundary condition becomes

$$\tilde{\psi}_{\mathcal{S}\lambda}(0) = 0, \qquad \tilde{\psi}_{\mathcal{S}\lambda}(x_{opt}) = \phi(x_{opt}).$$

Therefore, the optimal control of semelparous species, $\tilde{v}_{\mathcal{S}}(x)$, becomes a Markovian control, such that

$$\tilde{v}_{\mathcal{S}}(X_a) = \tilde{v}(x_{opt}, X_a). \tag{9.9}$$

As shown in the above equation, the optimal control does not depend on age.

9.2 Optimal growth in iteroparous species

Since iteroparous species reproduce during their growth, the value function becomes

$$\begin{aligned}\tilde{\psi}_{\mathcal{I}\lambda}(x) :&= \sup_{v\in\mathcal{V}} \int_0^{\infty} da \exp\{-\lambda a\} \mathbb{E}_x^v \left[F_{\mathcal{I}}(X_a) S_{\mathcal{I}}(a)\right] \\ &= \sup_{v\in\mathcal{V}} \int_0^{\alpha} da \exp\{-\lambda a\} \mathbb{E}_x^v \left[F_{\mathcal{I}}(X_a) S(a)\right]. \end{aligned} \tag{9.10}$$

Therefore, iteroparous species should optimize not only mortality but also fertility. In other words, the evolution of iteroparous species implies the temporary optimization of the ERS. Moreover, the maximum age, α, provides a terminal condition to the ERS, which introduces complexity to the analysis of iteroparous species.

To analyze the value function, Eq.(9.10), we introduce the ERS with $\exp\{-\lambda a\}$

$$w_{\lambda,a}(x) := \exp\{-\lambda a\} \mathbb{E}_x^v \left[F_{\mathcal{I}}(X_a) S(a)\right], \tag{9.11}$$

and a new value function described by backward age

$$\tilde{w}_{\lambda,a}(x) := \sup_{v\in\mathcal{V}} \exp\{-\lambda(\alpha - a)\} \mathbb{E}_x^v \left[F_{\mathcal{I}}(X_{\alpha-a}) S(\alpha - a)\right], \tag{9.12}$$

to use the following relationship:

$$\tilde{w}_{\lambda,0}(x) = \sup_{v\in\mathcal{V}} \left\{ \exp\left\{-\lambda a\right\} \mathbb{E}_x \left[\tilde{w}_{\lambda,a}(X_a) S(a) \right] \right\}. \tag{9.13}$$

This equation implies $\sup_{v\in\mathcal{V}} w_{\lambda,a}(x)$ corresponding with $\tilde{w}_{\lambda,0}(x)$ by using Eq.(9.12) (the Bellman principle). $\tilde{w}_{\lambda,0}(x)$ is the value function at age α in the original variable of a. Then, Eq.(9.10) is rewritten as

$$\tilde{\psi_{\mathcal{I}\lambda}}(x) = \int_0^\alpha da\, \tilde{w}_{\lambda,a}(x). \tag{9.14}$$

We obtain the optimal control by using Eq.(9.12). To analyze the dynamics of Eq.(9.12), we formally apply the Feynman–Kac formula (Appendix B) to Eq.(9.10), and the HJB equation becomes

$$\begin{cases} \dfrac{\partial}{\partial a}\tilde{w}_{\lambda,a}(x) - \inf\limits_{v\in\mathcal{V}} \left\{ \bar{\mathcal{H}}_x^v + \lambda \right\} \tilde{w}_{\lambda,a}(x) = 0 \\ \tilde{w}_{\lambda,\alpha}(x) = F_{\mathcal{I}}(x). \end{cases} \tag{9.15}$$

Then, the above equation suggests that an optimal control for iteroparous species $\tilde{v}_{\mathcal{I}}(a,x)$ depends not only on size, x, but also on age, a. Therefore, an iteroparous species with the optimal growth rate using original age (age forward), a, becomes

$$\begin{cases} d\tilde{X}_a = g\left(\tilde{X}_a, \tilde{v}_{\mathcal{I}}\left(\alpha - a, \tilde{X}_a\right)\right) da + \sigma\left(\tilde{X}_a, \tilde{v}_{\mathcal{I}}\left(\alpha - a, \tilde{X}_a\right)\right) dB_a \\ \tilde{X}_0 = x, \end{cases} \tag{9.16}$$

from Eq.(7.1). Since Eq.(9.16) is not an autonomous system, a projection function of the optimal growth in the population vector should be extended to

$$\tilde{P}_t\left(a,y\right)=\begin{cases} n_{t-a}\left(x\right)\tilde{K}_{a\in(0,\alpha)}\left(x\rightarrow y\right) & a<\alpha \\ 0 & a\geq\alpha \end{cases} \tag{9.17}$$

from Eq.(7.5) and

$$\begin{cases} \tilde{K}_{a\in(0,\alpha)}\left(x\rightarrow y\right)= \\ \quad\int_{\tilde{X}_0=x}^{\tilde{X}_a=y}\mathcal{D}\left(x\right)\int_{-\infty}^{\infty}\mathcal{D}\left(q\right)\exp\left\{\int_0^a d\tau\left(-iq_\tau\dot{\tilde{X}}_\tau-\tilde{\mathcal{H}}\left(\tau,-iq_\tau,\tilde{X}_\tau\right)\right)\right\} \\ \tilde{\mathcal{H}}\left(\tau,-iq_\tau,\tilde{X}_\tau\right):=-iq_\tau\tilde{g}\left(\tau\tilde{X}_\tau\right)+q_\tau^2\tilde{\sigma}\left(\tau,\tilde{X}_\tau\right)^2+\tilde{\mu}\left(\tau,\tilde{X}_\tau\right), \end{cases} \tag{9.18}$$

or

$$\begin{cases} \tilde{K}_{a\in(0,\alpha)}\left(x\rightarrow y\right)=\int_{\tilde{X}_0=x}^{\tilde{X}_a=y}\mathcal{D}\left(x\right)\exp\left\{\int_0^a d\tau\tilde{\mathcal{L}}\left(\tau,\dot{\tilde{X}}_\tau,\tilde{X}_\tau\right)\right\} \\ \tilde{\mathcal{L}}\left(\tau,\dot{\tilde{X}}_\tau,\tilde{X}_\tau\right):=-\dfrac{\left(\dot{\tilde{X}}_\tau-\tilde{g}\left(\tau,\tilde{X}_\tau\right)\right)^2}{2\tilde{\sigma}\left(\tau,\tilde{X}_\tau\right)^2}-\tilde{\mu}\left(\tau,\tilde{X}_\tau\right), \end{cases} \tag{9.19}$$

where

$$\begin{aligned} \tilde{g}\left(a,\tilde{X}_a\right) &:= g\left(\tilde{X}_a,\tilde{v}_{\mathcal{I}}\left(\alpha-a,\tilde{X}_a\right)\right) \\ \tilde{\sigma}\left(a,\tilde{X}_a\right) &:= \sigma\left(\tilde{X}_a,\tilde{v}_{\mathcal{I}}\left(\alpha-a,\tilde{X}_a\right)\right) \\ \tilde{\mu}\left(a,\tilde{X}_a\right) &:= \mu\left(\tilde{X}_a,\tilde{v}_{\mathcal{I}}\left(\alpha-a,\tilde{X}_a\right)\right). \end{aligned} \tag{9.20}$$

Then, the derivation of the extended path-integral is shown in Appendix E. Consequently, an Euler–Lotka equation composed of Eq.(9.10) provides the fitness of the population vector, Eq.(9.17).

9.3 Density of breeding age structure in fittest population structures

If we can obtain the fittest BRN, ERS, and cumulant generating function of breeding age directly from the value function, as for an objective function, analyzing the fittest population structure is useful. When one applies Eq.(9.10) to Eq.(5.4) as an objective function in the optimal control, Eq.(9.10) should be a Laplace transform of the ERS. This means that the optimal control should not be a function of λ because expanding the logarithm of Eq.(9.10) into a Taylor series with respect to $-\lambda$ causes a loss of the meaning of the objective function in the optimal control. This holds true as long as maximizing the ERS is equivalent to maximizing fitness. The key point to calculate in the case is the second term of the RHS of another expression of the value function, Eq.(9.12):

$$\tilde{w}_{\lambda,a}(x) = F_{\mathcal{I}}(x) - \inf_{v\in\mathcal{V}} \mathbb{E}_x \left[\int_0^{\alpha-a} d\tau \left\{ \bar{\mathcal{H}}_x^v + \lambda \right\} \exp\left\{-\lambda\tau\right\} F_{\mathcal{I}}(X_\tau) S(\tau) \right], \tag{9.21}$$

obtained by integrating both sides of Eq.(9.15) for age a (Dynkin's formula [12]). Differentiating the integrant of the second term in Eq.(9.21) with

respect to v, we obtain the condition that v^* satisfies:

$$\nabla_v \left\{\bar{\mathcal{H}}_x^v + \lambda\right\} \exp\left\{-\lambda\tau\right\} F_{\mathcal{I}}\left(X_\tau\right) S\left(\tau\right)\Big|_{v=v^*}$$
$$= \nabla_v \left(\bar{\mathcal{H}}_x^{v^*} F_{\mathcal{I}}\left(X_\tau\right)\right) - \left\{\bar{\mathcal{H}}_x^{v^*} + \lambda\right\} F_{\mathcal{I}}\left(X_\tau\right) \int_0^\tau ds \nabla_v \mu\left(X_s, v^*\right) = 0, \tag{9.22}$$

where $\nabla_v := \sum_{j=1}^d \partial/\partial v_j$. This equation shows that the optimal control does not depend on λ if and only if the mortality does not include the control vector. In other words, deriving the optimal control maximizing the ERS from Eq.(9.21) without calculating the Euler–Lotka equation directly is sufficient in this case. From a biological point of view, individuals of the species do not control their life spans in this case. In general, an optimal control optimizes the ERS and life span because prolificacy and precocity increase the fitness in r-selection [31, 32]. In other words, v^* being unconnected to λ means excluding the control of precocity. Then, the value functions can directly compose the cumulant generating function of breeding age $a^\diamond$ in the fittest population structure such that

$$\tilde{\Theta}_\lambda\left(x\right) := \log \tilde{\psi}_{\mathcal{I}\lambda}\left(x\right)$$
$$= \sum_{l=0}^\infty \frac{\left(-\lambda\right)^l}{l!} \langle \tilde{a^\diamond} \rangle_x^{(l)}, \tag{9.23}$$

and

$$\langle \tilde{a^{\diamond}} \rangle_{x}^{(l)} := \lim_{\lambda \to 0} \left[(-1)^{l} \frac{\partial^{l}}{\partial \lambda^{l}} \tilde{\Theta}_{\lambda} (x) \right]. \tag{9.24}$$

By using the original age, the density of $a^{\diamond}$ in the fittest population structure is given by the following function:

$$\mathbb{A}_{\mathcal{I}} (a) := \lim_{\lambda \to 0} \frac{\tilde{w}_{\lambda, \alpha - a} (x)}{\tilde{\psi}_{\mathcal{I}\lambda} (x)}, \tag{9.25}$$

where $\tilde{\psi}_{\mathcal{I}_0} (x)$ means BRN.

In the next section, we examine several specific models in semelparous and iteroparous breeding systems and discuss their differences.

Part IV
Application of OLSP to semelparous species

In this section, we give applications of the theory of this study for semelparous and iteroparous species using simple specific models. We show that the convexity of the objective function provides a measure of the susceptibility of a species to internal stochasticity, while the diversity of resources is important for species with low convexity of the objective function.

10 A simple stochastic model of a semelparous species

In this section, we examine a simple and specific stochastic model of a semelparous species. We apply the method used in previous sections to the model and examine how stochasticity affects life history and population growth. First, we define specific functions in the life history as in section 1 and show the characteristics of stochastic growth by using the Lagrangian in Eq.(3.16). Second, we derive the objective function, the fitness, and the optimal schedule from the life history. Then, we estimate a threshold of persistence for

a species with optimal schedule and examine the effects of stochasticity on fitness. Third, we analyze the effects of stochasticity on reproduction by deriving the BRN and statistics of mature age obtained from the cumulant generating function. Finally, we derive the mature age density and estimate the effects of stochasticity on life history by comparison with the density and BRN.

10.1 Assumption of the model

We consider an application of the optimal schedule problem by using a simple assumption of the size growth process:

$$\begin{aligned} g(y) &= \gamma y \\ \sigma(y) &= \sigma_0 y, \end{aligned} \tag{10.1}$$

where γ and σ_0 are nonnegative constants in Eq.(1.1). Eq.(10.1) describes an exponential size growth with fluctuation, which is like simple cell division, until the mature age, a^*. Eq.(10.1) is called geometric Brownian motion, and is well known as a stock price fluctuation model in mathematical finance [33]. The Black–Scholes model is especially renowned as the pricing model of options [34], which uses that SDE. Furthermore, we assume mortality in Eq.(6.2), such that

$$\mu(y) = const.,$$

where we set

$$\mu(y) = \mu_0. \tag{10.2}$$

10.2 Analysis of the growth curve using the Lagrangian

Applying the transformation of Eq.(3.10) to Eq.(10.1) ($\kappa = \sigma_0$ and $\nu(y) = y$), the Langragian of the model becomes

$$\tilde{\mathcal{L}}\left(\dot{Z}_\tau, Z_\tau\right) = -\frac{1}{2{\sigma_0}^2}\left[\dot{Z}_\tau - \left(\gamma - \frac{{\sigma_0}^2}{2}\right)\right]^2 - \mu_0, \tag{10.3}$$

from Eq.(3.16). Since mortality is constant, the mass of body size can be assumed to be concentrated around the dynamic system $\dot{Z}_\tau = (\gamma - {\sigma_0}^2/2)$. Therefore, the median of the size transition dynamics in a cohort, $\bar{X}_a$, is proportional to

$$\bar{X}_a \propto \exp\left\{\left(\gamma - \frac{{\sigma_0}^2}{2}\right)a\right\}. \tag{10.4}$$

This means that a characteristic of geometric Brownian motion is that the X_a almost certainly converges to zero if $\gamma < \frac{{\sigma_0}^2}{2}$ and diverges if $\gamma > \frac{{\sigma_0}^2}{2}$ for each sample path in the limit, $a \to \infty$. Under the former condition, it is possible for individuals never to reach the mature age, even if mortality (μ_0) is equal to zero [12]. This property is inherent in the diffusion process.

10.3 Optimal strategy and the persistence of species

The steady state of the population vector in juveniles $P_t^{\dagger}(a, y)$ is given by

$$P_t^{\dagger}(a, y) = Q_x \exp\left\{\lambda^*_{x^*,x}(t-a)\right\} K_a\left(x \to y \middle| y < x^*\right).$$

Q_x and $K_a\left(x \to y \middle| y < x^*\right)$ are analytically solvable (Appendix F).

Using the adjoint Hamiltonian of the differential form

$$\bar{\mathcal{H}}_x = -\gamma x \frac{d}{dx} - \frac{1}{2}\sigma_0^2 x^2 \frac{d^2}{dx^2} + \mu_0, \tag{10.5}$$

we can obtain $\psi_{\lambda,x^*}(x)$ by solving Eq.(5.2) at $x < x^*$ (Appendix.E) as follows:

$$\begin{aligned} \psi_{\mathcal{S}\lambda,x^*}(x) &= \left(\frac{x}{x^*}\right)^{\rho_\lambda} \phi(x^*) \\ \rho_\lambda &:= \frac{1}{2}\left(1 - \frac{2\gamma}{{\sigma_0}^2}\right) + \frac{1}{2}\sqrt{\left(1 - \frac{2\gamma}{{\sigma_0}^2}\right)^2 + \frac{8\mu_0}{{\sigma_0}^2} + \frac{8\lambda}{{\sigma_0}^2}}. \end{aligned} \tag{10.6}$$

ρ_λ shows that the domain of λ is

$$-\mu_0 - \frac{{\sigma_0}^2}{8}\left(1 - \frac{2\gamma}{{\sigma_0}^2}\right)^2 < \lambda < \infty. \tag{10.7}$$

The domain provides the lower limit of population growth. Using Eq.(10.6), we can solve Eq.(4.6) and obtain the fitness $\lambda^*_{x^*}$, which is a dominant characteristic root of Eq.(4.6) as follows:

$$\lambda^*_{x^*} = \left[\frac{{\sigma_0}^2}{2}\frac{\log\phi(x^*)}{\log\frac{x^*}{x}} + \left(\gamma - \frac{{\sigma_0}^2}{2}\right)\right]\frac{\log\phi(x^*)}{\log\frac{x^*}{x}} - \mu_0. \tag{10.8}$$

Since $\log \phi(x^*) / \log [x^*/x]$ is always positive due to $\phi(x^*) > 1$ and $x^* > x$, $\lambda^*_{x^*}$ is at its maximum when $\log \phi(x^*) / \log [x^*/x]$ is at its maximum. Therefore,

$$\lambda^*_{opt} = \left[\frac{{\sigma_0}^2}{2} m + \left(\gamma - \frac{{\sigma_0}^2}{2} \right) \right] m - \mu_0, \tag{10.9}$$

where

$$m = \frac{\log \phi\left(x^*_{opt}\right)}{\log \frac{x^*_{opt}}{x}}. \tag{10.10}$$

For the persistence of the species ($\lambda^*_{opt} \geq 0$), m should be larger than ρ_0. For example,

$$\phi(y) = \frac{Ry^l}{{x_c}^l + y^l} \tag{10.11}$$

($R > 1$, $x_c > 0$ and $l \geq 1$) has an optimal schedule (see Fig. 2). Analyzing the sensitivity of λ^*_{opt} with respect to the magnitude of stochasticity (σ_0^2), since m is always positive at any x^*_{opt}, we have

$$\frac{\partial}{\partial {\sigma_0}^2} \lambda^*_{opt} = \frac{1}{2} (m-1) m, \tag{10.12}$$

and obtain

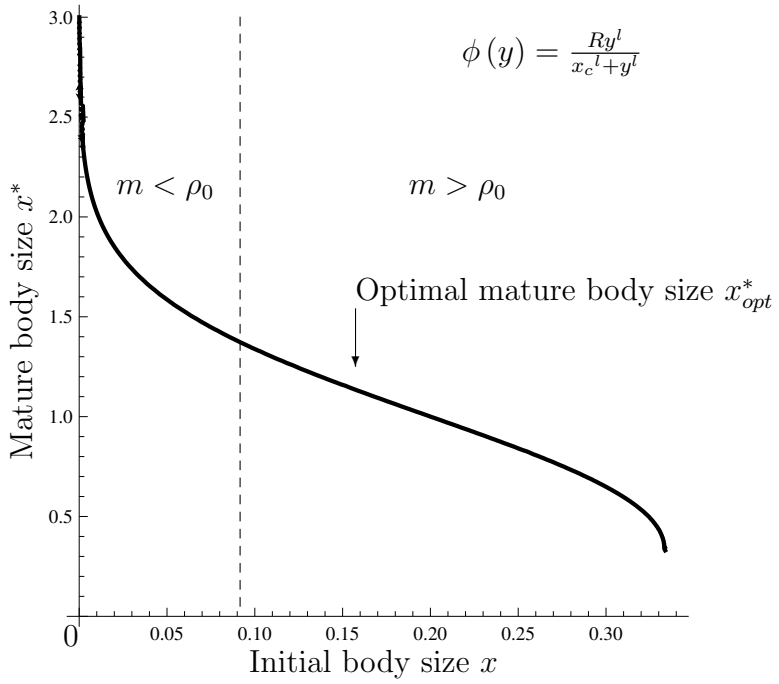

Figure 2: An example of an optimal schedule. This figure shows that each individual initial body size has its own optimal mature body size and this determines whether the species is persistent. We use $\phi(y)$ in Eq.(10.11) as an example. The species never survives when the initial body size is below the dashed line in the figure. The intersection between the dashed line and the curve of optimal mature body size is equal to $x^*_{opt} = x_c (l/\rho_0 - 1)^{1/l}$, which maximizes $\psi_{\mathcal{S}0,x^*}(x)$ with respect to x^*. The parameters used are $\gamma = 0.1$, $\sigma_0 = 0.5$, $\mu_0 = 0.04$, $R = 10.0$, $x_c = 1.0$, and l=2.0.

$$\frac{\partial}{\partial {\sigma_0}^2}\lambda^*_{opt} < 0, \qquad (m < 1) \tag{10.13a}$$

$$\frac{\partial}{\partial {\sigma_0}^2}\lambda^*_{opt} = 0, \qquad (m = 1) \tag{10.13b}$$

$$\frac{\partial}{\partial {\sigma_0}^2}\lambda^*_{opt} > 0, \qquad (m > 1)\,. \tag{10.13c}$$

The internal stochasticity negatively affects fitness in the case of Eq.(10.13a), but positively affects fitness in the case of Eq.(10.13c). Therein lies the main difference between internal and external stochasticity, as the latter always exhibits negative effects.

To consider why different values of m generate the contrasting effects, we must reveal the relationship between the BRN, $\psi_{\mathcal{S}_{0,x^*}}(x)$, and the mature age, a^*.

10.4 Basic reproductive number and mature age

Since fertility and maturity are important factors in population growth, we examine how these two factors affect fitness in the optimal life schedule. As mentioned previously, we focus on the effects of internal stochasticity on the BRN as the following:

$$\psi_{\mathcal{S}_{0,x^*}}(x) = \left(\frac{x}{x^*}\right)^{\rho_0} \phi(x^*)\,, \tag{10.14}$$

from Eq.(10.6). Using Eq.(10.10) and substituting x^*_{opt} into x^*, Eq.(10.14) becomes the BRN in the optimal body size as follows:

$$\psi^*_{\mathcal{S}0} := \phi\left(x^*_{opt}\right)^{1-\frac{\rho_0}{m}}. \tag{10.15}$$

Then, the effects of stochasticity on the BRN depend on whether m is greater or less than 1 (see Fig. 3). To understand the behavior of the BRN with internal stochasticity, the key point is the value of ρ_0. ρ_0 with deterministic growth and high stochasticity are

$$\lim_{\sigma_0 \to 0} \rho_0 = \frac{\mu_0}{\gamma},$$

and

$$\lim_{\sigma_0 \to \infty} \rho_0 = 1,$$

respectively. Therefore, if m is greater than 1, a sufficiently large stochasticity can conserve "$1 - \rho_0/m$" as positive, and hence make the species persist because of $\phi\left(x^*\right) > 1$ and the BRN¿1. If m is less than 1, the species could go extinct with increased stochasticity. Note that ρ_0 is a monotonic function with respect to σ_0.

Increased stochasticity could save a species from extinction in $m > 1$ even if μ_0/γ is larger than m, i.e., the BRN at $\sigma_0 = 0$ is less than 1 (see Fig.

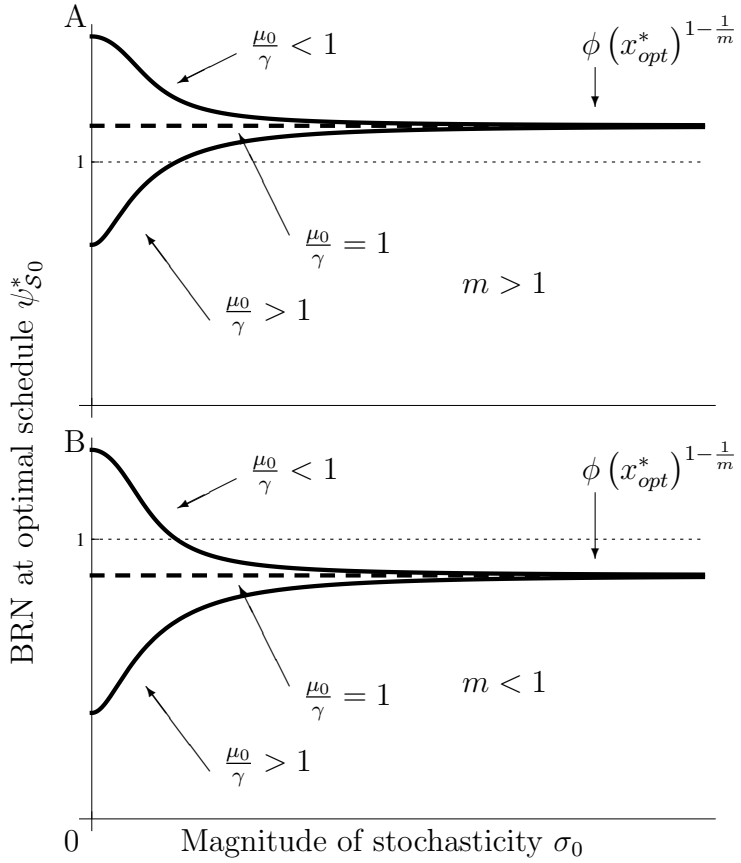

Figure 3: Behavior of the BRN with different magnitudes of stochasticity. This figure illustrates different behaviors of the BRN with respect to σ_0 in response to the condition of $\phi\left(x^*_{opt}\right)$ in inequality Eq.(10.13). Fig. A shows that that increases in σ_0 never cause extinction because the BRN exceeds 1 in $m > 1$. Fig. B shows that increases in σ_0 cause extinction or cause the population to be already in the process of becoming extinct at $m < 1$.

3A). Moreover, in comparison with the effect of mortality on ψ_0^*, the BRN decreases more rapidly with mortality in the deterministic case than in the stochastic case because the deterministic and stochastic environments have $\rho_0 = \mu_0/\gamma$ and $\rho_0 \approx \mu_0^{1/2}$ (see Eq.(10.6)), respectively. Stochasticity causes the species to persist with high mortality because it yields individuals that mature faster than they do under deterministic growth. Therefore, the ratio of μ_0/γ is an important factor determining whether offspring survivorship increases with internal stochasticity.

To explain the biological meaning of the result, one must analyze the effects of stochasticity on the mature age. When stochasticity affects the size growth process of each individual, the mature age has a variance and becomes statistics. We derive the cumulant generating function from Eq.(5.4), such that

$$\begin{aligned} \Theta_{\mathcal{S}\lambda}(x) &= \log \psi_{\mathcal{S}_{\lambda,x^*}}(x) \\ &= \log \phi(x^*) - \rho_\lambda \log \frac{x^*}{x}. \end{aligned} \tag{10.16}$$

From Eqs.(10.16) and (9.24), the expectation of mature age in deterministic growth is

$$\begin{aligned}\langle a^* \rangle_0^{(1)} &:= \langle a^* \rangle^{(1)} \Big|_{\sigma_0=0} \\ &= \frac{1}{\gamma} \log \frac{x^*}{x}, \qquad \left(\because \rho_0|_{\sigma_0=0} = \frac{\mu_0}{\gamma} \right) \end{aligned} \tag{10.17}$$

while that in stochastic growth is

$$\langle a^* \rangle^{(1)} = \frac{\log \frac{x^*}{x}}{\left[\left(\gamma - \frac{{\sigma_0}^2}{2} \right)^2 + 2\mu_0 {\sigma_0}^2 \right]^{\frac{1}{2}}}. \tag{10.18}$$

The expectation of mature age depends on stochasticity and mortality. Since a semelparous life span is identical to mature age, the effect of stochasticity on the life span depends on the following conditions:

$$\frac{\partial}{\partial {\sigma_0}^2} \langle a^* \rangle^{(1)} \leq 0, \qquad \left(\frac{{\sigma_0}^2}{4} + 2\mu_0 \geq \gamma \right) \tag{10.19a}$$

$$\frac{\partial}{\partial {\sigma_0}^2} \langle a^* \rangle^{(1)} > 0, \qquad \left(\frac{{\sigma_0}^2}{4} + 2\mu_0 < \gamma \right), \tag{10.19b}$$

from the derivative of Eq.(10.18) with respect to ${\sigma_0}^2$. If σ_0^2 or μ_0 is sufficiently large compared to γ, individuals with slower maturation contribute little to the expectation of mature age. Furthermore, the species as a whole has a short life span, as shown in [2, 35]. As a result, the expectation of mature age decreases compared to that under deterministic growth from the inequality

(10.19a). Conversely, when the parameters hold the inequality (10.19b), the expectation of mature age increases compared to that under deterministic growth. In other words, the expectation is affected by individuals with slower maturity.

From Eqs.(10.13c) and (10.19b) and Fig. 3A, we can consider a strange case, whereby stochasticity decreases the BRN and delays the expectation of mature age, while nevertheless increasing fitness. This occurs when the mortality is less than the growth rate constant $\mu_0/\gamma < 1$ and all parameters satisfy Eqs.(10.13c) and (10.19b). Then, the increased fitness appears to be a contradiction. A key to solving this contradiction lies in the characteristics of the mature age distribution. Therefore, we focus on the higher-order cumulant function to understand the shape of distribution.

Accordingly, the skewness should be evaluated as follows:

$$\begin{aligned} \langle a^* \rangle^{(3)} &= \lim_{\lambda \to 0} \left[(-1)^3 \frac{\partial^3}{\partial \lambda^3} \Theta_{\mathcal{S}\lambda}(x) \right] \\ &= \frac{3{\sigma_0}^4 \log \frac{x^*}{x}}{\left[\left(\gamma - \frac{{\sigma_0}^2}{2} \right)^2 + 2\mu_0 {\sigma_0}^2 \right]^{\frac{5}{2}}} > 0. \end{aligned} \tag{10.20}$$

This is definitely positive and shows that the distribution is biased toward a younger than expected age, suggesting that many individuals should attain

mature age faster than under deterministic growth. However, a small number of individuals with much slower maturity might affect this expectation. Due to the positive skewness, we must answer the important question of how far the mature ages are distributed from the deterministic ages. We derive and analyze the mature age structure of this model in the next section.

10.5 Mature age structure and maturity

To clarify the aforementioned issue, we analyze the mature age density in this section. From Eq.(5.1) and Eq.(6.2), we obtain the semelparous ERS, $u_{\mathcal{S}a}(x)$, as follows:

$$u_{\mathcal{S}a}(x) = \phi(x^*) \frac{\log \frac{x^*}{x}}{\sqrt{2\pi {\sigma_0}^2 a^3}} \exp\left\{ -\frac{\left[\log \frac{x^*}{x} - \left(\gamma - \frac{{\sigma_0}^2}{2}\right) a\right]^2}{2{\sigma_0}^2 a} - \mu_0 a \right\}, , \tag{10.21}$$

which is a kind of inverse Gaussian distribution (Appendix H). We have the semelparous mature age density $\mathbb{A}_{\mathcal{S}}(a)$ as follows:

$$\begin{aligned} \mathbb{A}_{\mathcal{S}}(a) &= \frac{u_{\mathcal{S}a}(x)}{\psi_{\mathcal{S}_{0,x^*}}(x)} \\ &= \frac{\log \frac{x^*}{x}}{\sqrt{2\pi\sigma_0^2 a^3}} \exp\left\{ -\frac{\left[\log \frac{x^*}{x} - \left(\gamma - \frac{\sigma_0^2}{2}\right) a\right]^2}{2{\sigma_0}^2 a} + \rho_0 \log \frac{x^*}{x} - \mu_0 a \right\}. \end{aligned} \tag{10.22}$$

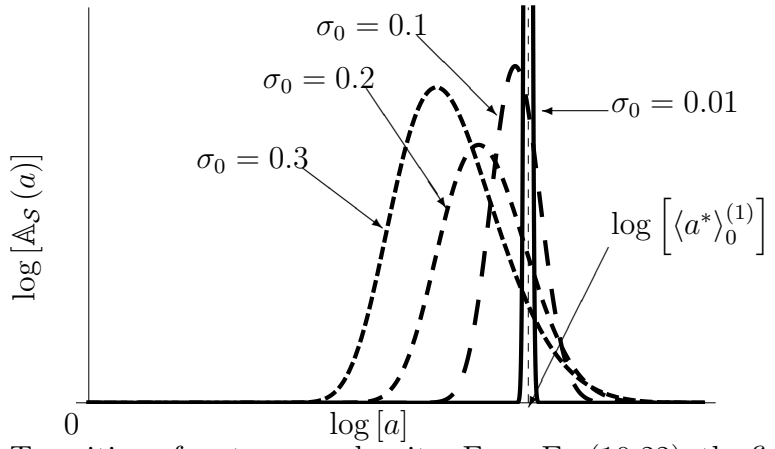

Figure 4: Transition of mature age density. From Eq.(10.22), the figure shows a transition of mature age density $\mathbb{A}_{\mathcal{S}}(a)$ with respect to σ_0 in a double logarithmic plot. Increases in σ_0 yield many individuals whose maturities are fast and a few individuals with slow maturity. In other words, higher stochasticity leads to many individuals with short life spans. Parameters are $\gamma = 0.1$, $\mu_0 = 0.04$, $x = 0.43$, $x^* = 0.9$ and $\sigma_0 = \{0.01, 0.1, 0.2, 0.3\}$.

To calculate the ratio of individuals whose maturity is faster than that under the deterministic model (Eq.(10.17)) numerically, we use the cumulative distribution function (CDF) as follows:

$$\mathbb{P}_{\mathcal{S}}\left[a^* \in (0, \langle a^* \rangle_0)\right] = \int_0^{\langle a^* \rangle_0} da \mathbb{A}_{\mathcal{S}}(a). \tag{10.23}$$

When σ_0 tends to zero, the inverse Gaussian distribution tends to the normal (Gaussian) distribution [36]. From these numerical calculations, we can see that the more stochasticity increases, the more individuals with faster maturity survive (see Figs. 4 and 5), while the right tail of the distribu-

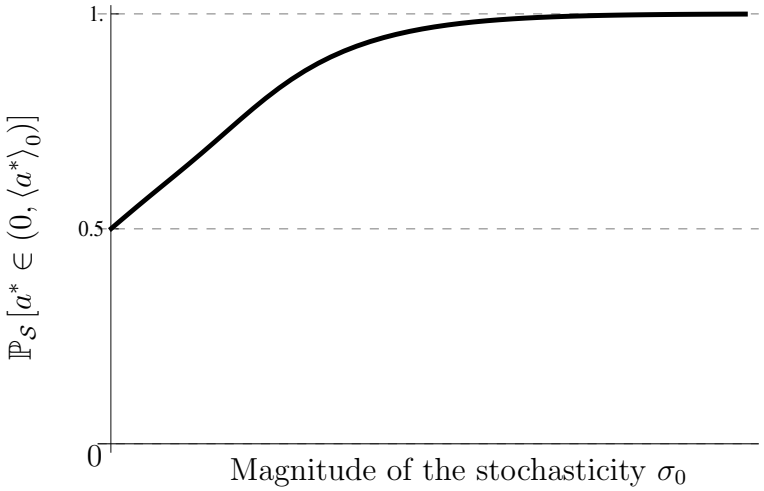

Figure 5: Proportion of mature individuals until age $\langle a^* \rangle_0$. The horizontal axis represents the magnitude of stochasticity, σ_0, and the vertical axis represents the proportion of already mature individuals before the deterministic mature age, which is given by CDF (10.23). It shows that in stochastic growth, high stochasticity increases the proportion of precocious individuals than under deterministic growth. The CDF always tends to exceed 50% at any parameter as a property of inverse Gaussian distribution. Therefore, environmental stochasticity necessarily causes short life spans. Parameters are the same as in Fig. 4.

tion increases (see Fig. 4) and yields the contribution of a few individuals with slower maturity to the expectation, as in Eq.(10.19b). However, the proportion of individuals maturing faster than under deterministic growth monotonically increases in Fig. 5.

Part V
Application to optimal risk aversion in the habitat

In the previous section, we showed that internal stochasticity could cause both increases and decreases in fitness. Focusing on the latter case, stochasticity represents a kind of risk for a species. Accordingly, in this section we show by the analysis of specific models that species which suitably avert the risk maximize their fitness in their habitat.

11 Two-resource utilization model

11.1 Assumptions of the model

Considering an extension of the simple model Eq.(10.1), we assume that the species can choose two kinds of resources (R_1 and R_2): a species using R_1 has the growth rate

$$\begin{cases} dX_{a,1} = \gamma_1 X_{a,1} da + \sigma_1 X_{a,1} dB_{a,1} \\ \\ X_{0,1} = x, \end{cases} \tag{11.1}$$

and a species using R_2 has the growth rate

$$\begin{cases} dX_{a,2} = \gamma_2 X_{a,2} da + \sigma_2 X_{a,2} dB_{a,2} \\ \\ X_{0,2} = x \end{cases} \tag{11.2}$$

where the parameters satisfy $\gamma_1 \in \mathbb{R}_+ > \gamma_2 \in \mathbb{R}$ (γ_2 could be negative), $\sigma_1 > \sigma_2 \geq 0$ i.e. choosing R_1 means a higher risk and higher expected growth rate than does choosing R_2. Conversely, choosing R_2 has another risk of individuals having lower survivorship until mature age than if they used R_1 because of their slower growth rate on average. Therefore, individuals should find an optimal "risk aversion" $\tilde{v} \in [0, 1]$ in the following growth rate:

$$\begin{cases} dX_a = [\gamma_1 (1 - v) + \gamma_2 v] X_a da + [\sigma_1 (1 - v) dB_{a,1} + \sigma_2 v dB_{a,2}] X_a \\ \\ X_0 = x, \end{cases} \tag{11.3}$$

to minimize the Hamiltonian with λ under the environment (see Fig. 6). Eq.(11.3) is well known as a typical "optimal portfolio selection problem" in mathematical finance and economics. Economists apply the problem to find an optimal investment of their wealth [37]. We assume mortality in Eq.(7.3), such that

$$\mu (y, v) = const.,$$

where we use the identical constant to that in Eq.(10.2) as follows:

$$\mu (y, v) = \mu_0 \tag{11.4}$$

independent of the control vector, v. We are interested in differences in the optimal utilization $\tilde{v}$ of Eq.(11.3) under different breeding systems. As a

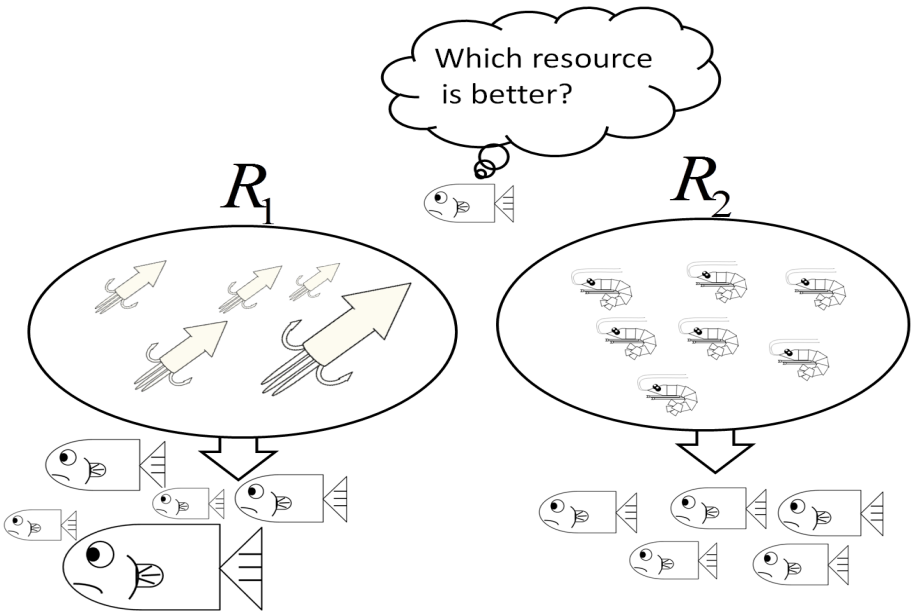

Figure 6: A resource utilization problem. This figure illustrates how a fish wavers in its choice. R_1 represents high risk but high expected growth rate, while both quantities are low in R_2. These resources fluctuate independently of each other. In other words, the two resources provide individuals with different internal stochasticities. The fish should optimally choose the best utilization of both resources.

preparation for analyzing the optimal utilization, the adjoint Hamiltonian of Eq.(11.3) becomes

$$\bar{\mathcal{H}}_x^v = -\left[\gamma_1 (1-v) + \gamma_2 v\right] x \frac{d}{dx} - \frac{1}{2}\left[(\sigma_1 (1-v))^2 + (\sigma_2 v)^2\right] x^2 \frac{d^2}{dx^2} + \mu_0. \tag{11.5}$$

Let $\varphi(x) \in C^2(\mathbb{R}_+)$ provide an extreme value of $\left\{\bar{\mathcal{H}}_x^v + \lambda\right\}\varphi(x)$ with respect to v, such that

$$\frac{\partial}{\partial v}\left\{\bar{\mathcal{H}}_x^v + \lambda\right\}\varphi(x)\Big|_{v=v^\dagger} = 0. \tag{11.6}$$

Then, the value satisfies

$$v^\dagger(\varphi(x)) = \frac{\sigma_1^2}{\sigma_1^2 + \sigma_2^2} + \frac{(\gamma_1 - \gamma_2)\frac{d}{dx}\varphi(x)}{(\sigma_1^2 + \sigma_2^2) x \frac{d^2}{dx^2}\varphi(x)}, \tag{11.7}$$

and we obtain a nonlinear operator by substituting Eq.(11.7) into (11.5) as follows:

$$\begin{aligned} H_\lambda(\varphi(x)) &:= \left\{\bar{\mathcal{H}}_x^v + \lambda\right\}\varphi(x)\Big|_{v=v^\dagger} \\ &= -\left[\frac{\gamma_1\sigma_2^2 + \gamma_2\sigma_1^2}{\sigma_1^2 + \sigma_2^2}\right] x \frac{\partial}{\partial x}\varphi(x) - \frac{1}{2}\frac{\sigma_1^2\sigma_2^2}{\sigma_1^2 + \sigma_2^2} x^2 \frac{\partial^2}{\partial x^2}\varphi(x) \\ &\quad + \frac{1}{2}\frac{(\gamma_1 - \gamma_2)^2\left(\frac{\partial}{\partial x}\varphi(x)\right)^2}{(\sigma_1^2 + \sigma_2^2)\frac{\partial^2}{\partial x^2}\varphi(x)} + (\mu_0 + \lambda)\varphi(x). \end{aligned} \tag{11.8}$$

Hereafter, we frequently use these equations, Eqs.(11.7) and (11.8), in analyses in this study.

11.2 Semelparous reproductive timing and optimal resource utilization

From the analysis of semelparous OLSP using Eqs.(10.1), (6.2), and (10.2), we use the optimal mature body size x^*_{opt} and m of Eq.(10.10) from part I V. Stochasticity was shown to decrease the fitness if, and only if, m is less than 1. In other words, the positive optimal utilization possibly exists at $m < 1$. If m is greater than 1, $\tilde{v}$ of Eq.(11.3) is obviously equal to zero because stochasticity positively affects fitness. In persistent species, large m is advantageous to species for any parameters.

From Eq.(9.8), the value function satisfying Eqs.(11.3), (6.2), and (10.2), $\tilde{\psi}_{\mathcal{S}\lambda}(x)$, is generated by the following HJB equation:

$$-\inf_{v\in\mathcal{V}}\left\{\bar{\mathcal{H}}^v_x+\lambda\right\}\tilde{\psi}_{\mathcal{S}\lambda}(x)+F_{\mathcal{S}}(x)=0. \tag{11.9}$$

Since Eq.(11.9) is a quadratic function of v (see Eq.(11.5)), the extreme value is uniquely determined by $v^\dagger\left(\tilde{\psi}_{\mathcal{S}\lambda}(x)\right)$ from Eq.(11.7). Substituting the value into Eq.(11.9), we obtain a nonlinear ODE as follows:

$$H_\lambda\left(\tilde{\psi}_{\mathcal{S}\lambda}(x)\right)+F_{\mathcal{S}}(x)=0, \tag{11.10}$$

from Eq.(11.8). To find the solution of Eq.(11.10) in the viscosity sense, we assume a solution $\tilde{\psi}_{\mathcal{S}\lambda}(x)=Cx^\rho$ $(C\neq 0)$, and substitute it into Eq.(11.10)

as follows:

$$\left[\left[\frac{\gamma_1\sigma_2^2+\gamma_2\sigma_1^2}{(\sigma_1^2+\sigma_2^2)}\right]\rho+\frac{1}{2}\frac{\sigma_1^2\sigma_2^2\rho\,(\rho-1)}{\sigma_1^2+\sigma_2^2}-\frac{1}{2}\frac{(\gamma_1-\gamma_2)^2\,\rho}{(\sigma_1^2+\sigma_2^2)\,(\rho-1)}-(\mu_0+\lambda)\right]Cx^{\rho}$$

$$=0. \tag{11.11}$$

Setting ρ_λ to satisfy Eq.(11.11), we obtain

$$\tilde{\psi_{\mathcal{S}\lambda}}(x)=\left(\frac{x}{x^*_{opt}}\right)^{\rho_\lambda}\phi\left(x^*_{opt}\right) \tag{11.12}$$

and the constant, C, is given by

$$\phi\left(x^*_{opt}\right){x^*_{opt}}^{-\rho_\lambda}$$

satisfying the boundary condition in Eq.(9.8). From the Euler-Lotka equation Eq.(7.8):

$$\left(\frac{x}{x^*_{opt}}\right)^{\rho_\lambda}\phi\left(x^*_{opt}\right)=\exp\left\{\log\phi\left(x^*_{opt}\right)-\rho_{\tilde{\lambda}}\log\frac{x^*_{opt}}{x}\right\}=1,$$

$\tilde{\lambda}$ should hold the following relationship

$$\rho_{\tilde{\lambda}}=m, \tag{11.13}$$

from Eq.(10.10). Considering $m<1$, we can find the optimal control from Eq.(11.7), because the value function, $\tilde{\psi_{\mathcal{S}\lambda}}(x)$, becomes a concave function.

Substituting Eqs.(11.12) and (11.13) into Eq.(11.7), the optimal utilization, $\tilde{v}_S$, becomes

$$\tilde{v}_{\mathcal{S}}(x)=\max\left\{\frac{\sigma_1^2}{\sigma_1^2+\sigma_2^2}-\frac{\gamma_1-\gamma_2}{(\sigma_1^2+\sigma_2^2)\,(1-m)},0\right\}. \tag{11.14}$$

The optimal utilization provided by the $\tilde{v}_{\mathcal{S}}$ is a constant, and it means that the species should conserve a proportion of resources during its lifetime. Regarding $\tilde{v}_{\mathcal{S}}$ as a function of m, m is an important index to determine utilization. If the index is large, it shows that the semelparous species has a tendency toward risk appetite (see Fig. 7) because $\tilde{v}_S$ is small. Then, the optimal resource utilization continuously changes with respect to m. Since the continuity of optimal control with respect to m is provided by the second-order term of v in the diffusion term of the Hamiltonian, Eq.(11.5), it is different from the bang–bang controls appearing in deterministic models, which do not have second-order terms of control parameters. From Eqs.(10.9), (11.11), and (11.13), we obtain the fitness of the fittest as follows:

$$\tilde{\lambda}_{\mathcal{S}}(m) = \begin{cases} m\left[\frac{{\sigma_1}^2}{2}m + \left(\gamma_1 - \frac{{\sigma_1}^2}{2}\right)\right] - \mu_0 & \text{if} \quad \tilde{v}_S(m) = 0 \\ m\left[\frac{\gamma_1\sigma_2^2+\gamma_2\sigma_1^2}{\sigma_1^2+\sigma_2^2} - \frac{1}{2}\frac{\sigma_1^2\sigma_2^2(1-m)}{\sigma_1^2+\sigma_2^2} + \frac{1}{2}\frac{(\gamma_1-\gamma_2)^2}{\left(\sigma_1^2+\sigma_2^2\right)(1-m)}\right] - \mu_0 & \text{if} \quad 0 < \tilde{v}_S(m) < 1 \end{cases}, \tag{11.15}$$

from the LHS of Eq.(11.11) (see Fig. 8). If $\tilde{\lambda}_{\mathcal{S}}(m)$ is nonnegative, the species is persistent. In that case, the fittest option is to be an R_1-specialist or generalist, and an R_2-specialist is never selected for because of the magnitude correlation of each parameter in the definition of this study. Nature selects

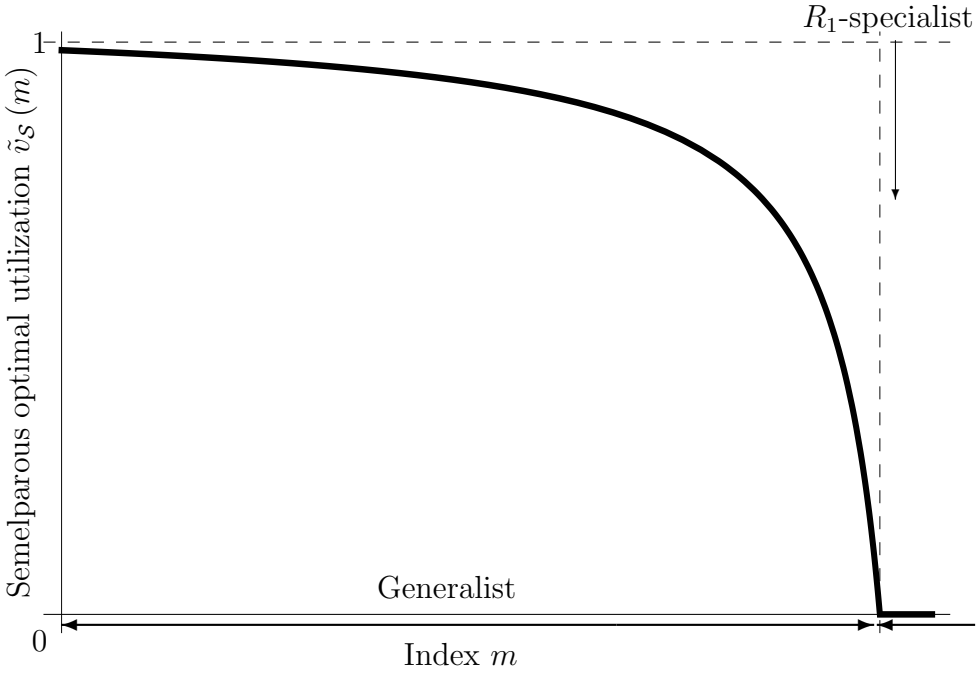

Figure 7: Semelparous optimal utilization for each m. This figure shows the semelparous optimal resource utilization, Eq.(11.15), depending on m. Two different types of feeding habitat exist. A small or intermediate value of $m \in \left(0, 1 - \frac{1}{\sigma_1^2}(\gamma_1 - \gamma_2)\right)$ makes the species a generalist: the larger the value of m, the more the species favors risk and becomes specialist. Parameters are $\gamma_1 = 0.16$, $\gamma_2 = 0.1$, $\sigma_1 = 1.0$, $\sigma_2 = 0.12$, and $\mu_0 = 0.01$.

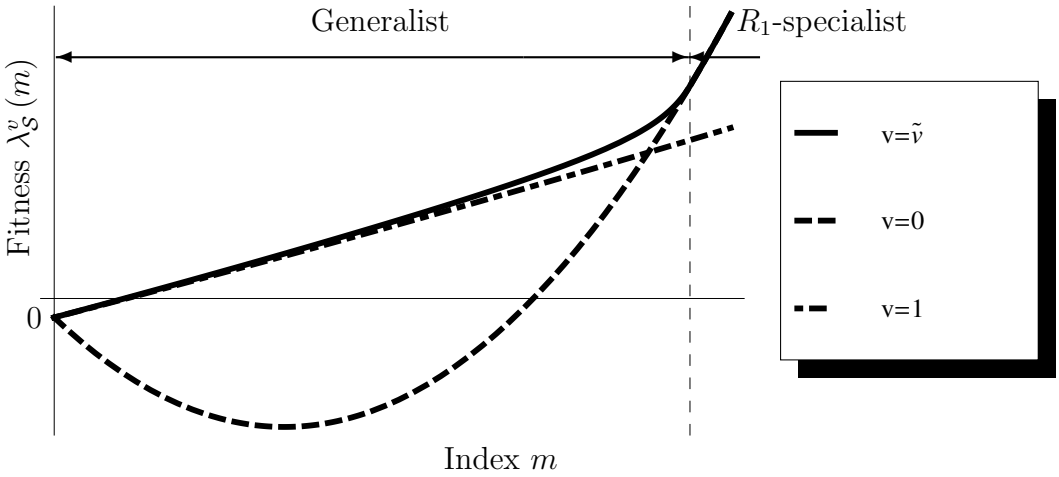

Figure 8: Fitness of optimal utilization in semelparous species: We calculate the value of the fitness of semelparous species with respect to m between zero and 1. The vertical dashed line represents the boundary between specialists and generalists as given by Eq.(11.16). The fitness is always a monotonically increasing function of m in the persistent region of the species ($\tilde{\lambda}_{\mathcal{S}}(m) \geq 0$). It is remarkable that a large m causes individuals to favor risk and increase their fitness. This figure shows the optimal resource utilization actually having advantages over specialists of each of the resources. Parameters are the same as in Fig. 7.

a generalist when m is within

$$0 < m < 1 - \frac{1}{\sigma_1^2}(\gamma_1 - \gamma_2), \tag{11.16}$$

otherwise an R_1-specialist is selected. The dependence of utilization on m can be explained by a trade-off between the generation cycle and the BRN. In part IV, we showed that internal stochasticity increases the number of precocious individuals and decreases the number of mature individuals. A large

value of m expresses a small difference between the mature body size and initial body size and/or high fertility $\phi\left(x_{opt}^{*}\right)$ and causes the reproduction number of precocious individuals to compensate for the decrease in the number of mature individuals. Small values of m cause the opposite, whereby the reduction in the number of mature individuals exceeds the reproductive output of precocious individuals (see Figs. 9 and 10).

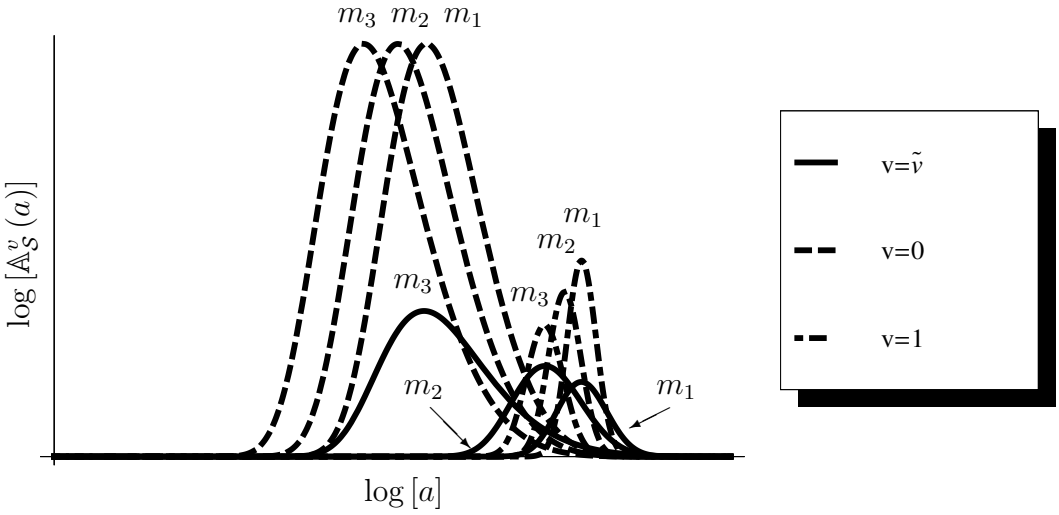

Figure 9: Transition of the mature age distribution. Whenever m becomes large ($m_1 < m_2 < m_3$), the mature age distributions of every utilization behavior are shifted to younger ages than those under smaller m as in [11]. If the fittest species is a generalist, the change in distribution becomes extreme. Then, the age distribution is provided by Appendix I. We chose $\phi(y) = Ry^l/\left(x_c^l + y^l\right)$ as the fertility rate function. This function has a unique m with respect to x, and the optimal body size, x^*_{opt}, is obtained by calculating the derivative of $\left(\log\left[\phi\left(x^*_{opt}\right)\right]/\log\left[x^*_{opt}/x\right]\right)' = 0$ with respect to x^*_{opt}. We substitute the RHS of that equality into x of the distribution. Then, we obtain this figure by changing x^*_{opt}. Then, m becomes inversely proportional to x^*_{opt} in this fertility function. Parameters are $R = 10$, $x_c = 1.0$, $l = 2$, $x^*_{opt} = 1.1$, 1.3, 1.5, with the others being the same as in Fig. 8.

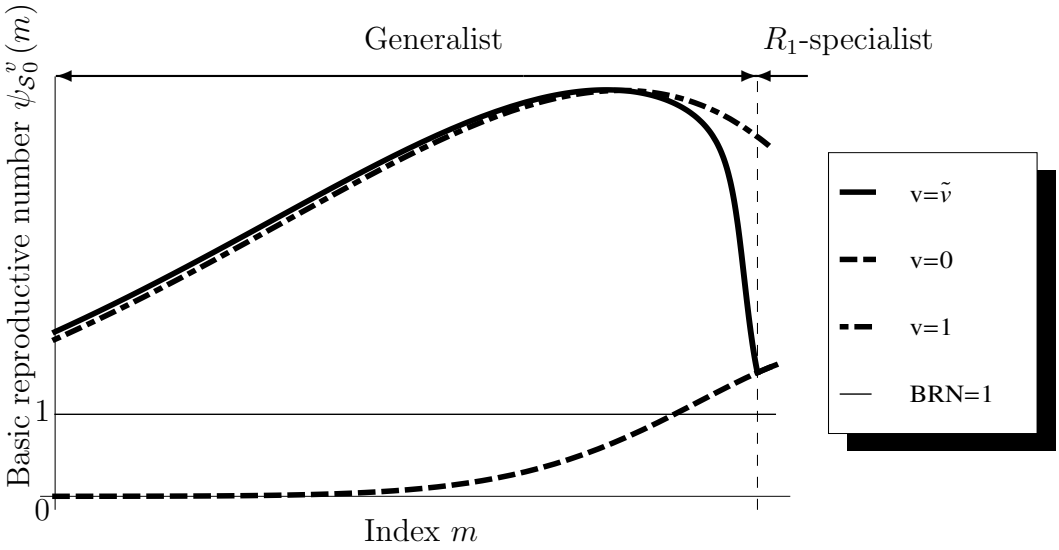

Figure 10: Transition of the BRN. This figure shows changes in the BRN with respect to m. The BRN of the fittest species increases as m increases; however, it decreases when m reaches the RHS of Eq.(11.16), which means that the growth strategy changes from the conservation of the BRN to a hasty alternation of generation time. Utilizing R_1 usually, the BRN of the fittest is higher than that of $v = 0$. We simulate the BRN under the same parameters as in Fig. 9. To show the proportional connection between m and the BRN, we change the variable ($x^*_{opt} \to 3.5 - y$) and simulate it within (0, 3.5) because m is in inverse proportion to x^*_{opt}. Parameters are the same as in Fig. 9.

11.3 Iteroparous optimal utilization

In this subsection, changing from the breeding system of Eq.(6.2) to Eq.(7.2), we compare the optimal strategy of semelparity with that of iteroparity. We use the value function from Eqs.(9.10) and (9.12), and the same Hamiltonian as in Eq.(11.5).

We assume the fertility function to scale with body-size allometric law, such as for the biomass of shoots and body size in trees [38], as follows:

$$F_{\mathcal{I}\beta}(y) := by^{\beta} \qquad (0 < \beta < 1), \tag{11.17}$$

where b and β represent the fertility rate and an allometric exponent within the domain $(0, 1)$, respectively. Using the Hamiltonian, Eq.(11.5), we can obtain an optimal utilization of the iteroparous species identical to the one of the semelparous species. From Eqs.(9.15) and (11.7), the value function in Eq.(9.12), becomes a solution of the nonlinear PDE

$$\begin{cases} \dfrac{\partial}{\partial a}\tilde{w}_{\lambda,a}(x) - H_{\lambda}\left(\tilde{w}_{\lambda,a}(x)\right) = 0 \\ \tilde{w}_{\lambda,\alpha}(x) = bx^{\beta}, \end{cases} \tag{11.18}$$

because

$$H_{\lambda}\left(\tilde{w}_{\lambda,a}(x)\right) = \inf_{v\in\mathcal{V}}\left\{\bar{\mathcal{H}}_x^v + \lambda\right\}\tilde{w}_{\lambda,a}(x),$$

and the optimal utilization satisfies

$$\tilde{v}_{\mathcal{I}}(x) = \max\left\{\min\left\{v^{\dagger}\left(\tilde{w}_{\lambda,a}(x)\right), 1\right\}, 0\right\}, \tag{11.19}$$

from Eq.(11.7). To derive the solution of Eq.(11.18), we assume

$$\tilde{w}_{\lambda,a}(x) = \exp\left\{\eta_{\lambda}(\alpha - a)\right\} b x^{\beta}, \tag{11.20}$$

and substitute it into Eq.(11.18). Then, η_{λ} becomes

$$\eta_{\lambda} = \begin{cases} \beta\left[\frac{{\sigma_1}^2}{2}\beta + \left(\gamma_1 - \frac{{\sigma_1}^2}{2}\right)\right] - \mu_0 - \lambda & \text{if} \quad \tilde{v}_{\mathcal{I}}(\beta) = 0 \\ \beta\left[\frac{\gamma_1\sigma_2^2 + \gamma_2\sigma_1^2}{\sigma_1^2 + \sigma_2^2} - \frac{1}{2}\frac{\sigma_1^2\sigma_2^2(1-\beta)}{\sigma_1^2 + \sigma_2^2} + \frac{1}{2}\frac{(\gamma_1 - \gamma_2)^2}{\left(\sigma_1^2 + \sigma_2^2\right)(1-\beta)}\right] - \mu_0 - \lambda & \text{if} \quad 0 < \tilde{v}_{\mathcal{I}}(\beta) < 1 \end{cases}. \tag{11.21}$$

Eq.(11.20) is guaranteed as a unique solution of Eq.(11.18) from the uniqueness of the viscosity solution [39]. Namely, η_{λ} can be expressed by using the function of semelparous fitness, Eq.(11.15), such that

$$\eta_{\lambda} = \tilde{\lambda}_{\mathcal{S}}(\beta) - \lambda. \tag{11.22}$$

This suggests that the iteroparous optimal utilization has common and different characteristics compared to the semelparous one. We here use the expression, Eq.(11.22), to emphasize the common characteristics between semelparous and iteroparous optimal life histories. Substituting Eqs.(11.18)

and (11.21) into Eq.(11.19), we obtain the optimal utilization as follows:

$$\tilde{v}_{\mathcal{I}}(x) = \max\left\{\frac{\sigma_1^2}{\sigma_1^2+\sigma_2^2} - \frac{\gamma_1-\gamma_2}{(\sigma_1^2+\sigma_2^2)(1-\beta)}, 0\right\}, \tag{11.23}$$

without having to solve the Euler–Lotka equation, as the mortality does not include control parameters. When we regard the utilization, Eq.(11.23), as a function of β, the functional form resembles the optimal utilization of semelparous species, (Eq.(11.15)). Then, the exponent, β, plays the role of m in semelparous species.

Using Eqs.(9.10), (11.20), and (11.22), the iteroparous value function in Eq.(9.10) becomes

$$\tilde{\psi}_{\mathcal{I}\lambda}(x) = \int_0^\alpha da \exp\{\eta_\lambda(\alpha-a)\} bx^\beta = \frac{bx^\beta}{\eta_\lambda}\left(\exp\{\eta_\lambda\alpha\}-1\right). \tag{11.24}$$

Since the Euler–Lotka equation, Eq.(7.8), generated by Eq.(11.24) becomes transcendental, we cannot find the fitness of the iteroparous species explicitly. Then, we use the following inequality:

$$\tilde{\lambda}_I(\alpha,\beta) \leq \tilde{\lambda}_S(\beta) + bx^\beta, \tag{11.25}$$

where the RHS of Eq.(11.25) is the dominant characteristic root of

$$\lim_{\alpha\uparrow\infty} \tilde{\psi}_{\mathcal{I}\lambda^*}(x) = -\frac{bx^\beta}{\eta_{\lambda^*}} = 1$$

from the Euler–Lotka equation, Eq.(7.8), applying the "Basic optimal life schedule theorem" (Appendix C) to α. Since individuals in initial states normally contribute little to reproduction in nature, we roughly assume that bx^{β} is sufficiently small.

Considering the persistence of the species ($\tilde{\lambda}_{\mathcal{I}}(\alpha,\beta) \geq 0$), $\tilde{\lambda}_{\mathcal{S}}(\beta)$ should be nonnegative. In this model, the optimal utilization is supposed to maximize not only the fitness but also the ERS of the original age:

$$\tilde{w}_{0,a}(x) = \exp\left\{\tilde{\lambda}_{\mathcal{S}}(\beta)\, a\right\} bx^{\beta} \qquad a \in (0,\alpha) \tag{11.26}$$

Additionally, if the fitness, $\tilde{\lambda}_{\mathcal{I}}(\alpha,\beta)$, is a monotonically increasing function in β, β has an identical meaning to that of m in semelparous species. To prove this, we show that the ERS increases monotonically in β. Since $\tilde{\lambda}_{\mathcal{S}}$ satisfies

$$\frac{\partial}{\partial\beta}\tilde{\lambda}_{\mathcal{S}} > 0 \qquad {}^{\forall}\beta \in \{\varrho | 0 < \tilde{v}_I(\varrho) < 1\},$$

and Eq.(10.9) is a monotonically increasing function of m in $\lambda^{*}_{x_{opt}} \geq 0$, we conclude the proof.

From Eqs.(9.25) and (11.26) and the BRN:

$$\tilde{\psi_{\mathcal{I}_0}}(x) = \frac{bx^{\beta}}{\tilde{\lambda}_{\mathcal{S}}(\beta)}\left(\exp\left\{\tilde{\lambda}_{\mathcal{S}}(\beta)\,\alpha\right\} - 1\right), \tag{11.27}$$

the breeding age density becomes

$$\mathbb{A}_{\mathcal{I}}(a) = \begin{cases} \frac{\tilde{\lambda}_{\mathcal{S}}(\beta)\exp\left\{\tilde{\lambda}_{\mathcal{S}}(\beta)a\right\}}{\left(\exp\left\{\tilde{\lambda}_{\mathcal{S}}(\beta)\alpha\right\}-1\right)} & \tilde{\lambda}_{\mathcal{S}}(\beta) > 0 \\ \frac{1}{\alpha} & \tilde{\lambda}_{\mathcal{S}}(\beta) = 0. \end{cases} \tag{11.28}$$

The age density shows that if $\tilde{\lambda}_{\mathcal{S}}(\beta)$ is positive, the density skews toward older ages. In this case, the contribution of older individuals to reproduction is important for the persistence of the species. Even if $\tilde{\lambda}_{\mathcal{S}}(\beta)$ is equal to zero, the contribution is not negligible because the density has a uniform distribution. Since Eq.(11.15) maximizes the fitness of semelparous species, $\tilde{\lambda}_{\mathcal{S}}(m)$, the optimal utilization of iteroparous species also maximizes $\tilde{\lambda}_{\mathcal{S}}(\beta)$. Although for large values of m and β, species in both breeding types favor more risky behavior, their breeding age structures are different, such that the semelparous mature age density is L-shaped, while the iteroparous mature age density is J-shaped (see Fig. 9 and Eq.(11.28)). Consequently, the optimal utilization of iteroparous species enhances the contribution of older individuals to reproduction and differs from that of semelparous species because their longevity provides them with many opportunities for reproduction and with sufficient time to reach a large size.

Considering the persistence of the species ($\tilde{\psi}_{\mathcal{I}0}(x) \geq 1$) with respect to

the maximum age, α, the following relation should be satisfied:

$$\alpha \geq \frac{1}{\tilde{\lambda}_{\mathcal{S}}(\beta)} \log \left[1 + \frac{\tilde{\lambda}_{\mathcal{S}}(\beta)}{bx^{\beta}} \right], \tag{11.29}$$

from Eq.(11.27). Since Eq.(11.24) increases monotonically in α and Eq.(11.25) is proved by using the basic optimal life schedule theorem, iteroparous fitness is a monotonically increasing function in α. Therefore, iteroparous species evolve to have optimal utilization and to survive as long as possible, as found for trees.

Part VI
Discussion

12 Relationship with other LDMs (from part II)

The age-size structured model has three kinds of expression, TMM, PDE, and IPM. Takada and Hara (1994) showed a mathematical relationship between the expression of PDE and a TMM in a continuous limit by deriving Kramers–Moyal coefficients (see [15]) from the TMM [8]. Ellner introduced the IPM and Zuidema used it in his own analysis as the limit of the TMM [17, 18, 40]. Additionally, we show a relationship between PDE and IPM via path-integral expression. Therefore, these three expressions of the LDM have duality with each other and can be considered to draw the same picture in a biological context. Consequently, the analysis of internal stochasticity effects in this study might be applicable to other expressions of an age-size structured LDM.

If individuals are affected by internal stochasticity, we show that the fitness derived from the solution of a new Euler–Lotka equation (Eq.(4.6)) is identical to that of classic LDMs [25, 26]. Therefore, when we consider the op-

timal schedule in a life history, analyzing the objective function in stochastic growth is sufficient. This function gives us important quantities that characterize species, such as the BRN, ERS, and the cumulant generating function.

In semelparous species, we can analyze from the objective function further details of several quantities, such as the BRN and statistics of mature ages. The BRN is the product of the expectation of survivorship until a mature age and the reproductive number at mature body size (see Eq.(9.6)). Statistics on the mature age structure are provided by a cumulant generating function (see Eq.(5.4)), and the probability density is expressed by the ERS/BRN in stochastic growth. Using the generating function, we can analyze a characteristic of the life span. Thus, analysis of $\psi_\lambda(x)$ is a basic approach in age-size structured models with internal stochasticity.

We show that the optimal life schedule problem can be connected to population dynamics in stochastic growth. The connection is calculated by an age-size structured model with internal stochasticity. Then, the structure of the population vector is the product of the initial population (Eq.(4.5)) and the projection function (Eq.(3.2) or Eq.(3.3)), which is generated by life history and can be generally written as a path-integral expression. Al-

though we did not go into the details of the analysis of the path integral, the method connects the body-size transition in the population vector with a diffusion process of particles in physics, which allows us to use various analytical methods from physics and mathematics in stochastic growth.

13 OLSP and optimal growth process (from partⅢ)

Usually, OLSP in deterministic growth is an analysis of an optimal ratio of growing period to breeding period for a given life span [41, 42]. Then, a framework of Pontryagin's maximum principle is reasonable to analyze the OLSP. Although the framework is the necessary condition that the optimal schedule should satisfy, it has successfully and uniquely determined the optimal ratio in many species. The framework, however, is inadequate for species having variations in individual growth. Pontryagin's maximum principle should be extended to the stochastic Pontryagin's maximum principle for application to these kinds of species. Our approach is more reasonable than the framework in OLSP with internal stochasticity because the new framework includes variation in individual life spans and it can be simply rewritten as an application of the boundary value problem in a PDE (see

Eq.(5.1)), i.e., the optimal stopping problem. We then consider only the end of the growth period because we take into account variation in individual life spans. This framework gives us a way to analyze the evolution of the length of life spans, which cannot be analyzed in the framework of Pontryagin's maximum principle because one has to give a fixed life span according to the assumptions.

The analysis of optimal stochastic control using the HJB equation has been developed in various academic fields, including engineering and finance. However, many theoretical biologists have commonly used the "Maximum Principle" approach in the analysis of life schedules. The stochastic Maximum Principle is proved by Peng (1990) [43], but it is not overwhelmingly popular in theoretical biology. According to Yong and Zhou (1999) [44], both methods are formalized by the common Hamiltonian. Additionally, the correspondence of the HJB equation to the stochastic Maximum Principle was shown via the idea of a viscosity solution by mathematicians [39, 45, 46, 47]. They showed that the value function and its derivatives in the HJB equation corresponded to the costate variables in the stochastic Maximum Principle. The Hamiltonian, which mathematical biologists use in the Maximum

Principle approach, was merely one of the mathematical preparations for OLSP. The Hamiltonian now forms an important element of the demographic model. The path-integral formulation unifies stochastic control theory and LDMs via the Hamiltonian, and we showed that optimal strategies usually minimize $\bar{\mathcal{H}}_x^v + \lambda$. This Hamiltonian, $\bar{\mathcal{H}}_x^v$, forms a counterpart of the Fokker–Planck Hamiltonian, referred to as the "adjoint Hamiltonian" in Eq.(7.6). From a physical point of view, the Hamiltonian refers to the total energy of the system. Using this analogy, we can provide a biological meaning of the Hamiltonian, whereby individuals consume energy throughout their lifetime. Then, the value function derived from the HJB equation represents the lowest energy consumption over the lifetime, and the Euler–Lotka equation converts the life history into population dynamics. Therefore, we can omit the analysis of population dynamics in the LDM because the theory in this study showed that the following equations provide the unification of OLSP and LDM:

$$\begin{cases} -\inf\limits_{v\in\mathcal{V}} \left\{\bar{\mathcal{H}}_x^v + \lambda\right\} \tilde{\psi}_\lambda(x) + F(x) = 0 \\ \bar{\mathcal{H}}_x^v := -g(x,v)\dfrac{d}{dx} - \dfrac{1}{2}\sigma(x,v)^2 \dfrac{d^2}{dx^2} + \mu(y,v) \\ \tilde{\psi}_\lambda(x) = 1, \end{cases}$$

or another HJB equation:

$$\begin{cases} \dfrac{\partial}{\partial a}\tilde{w}_{\lambda,a}(x) - \inf\limits_{v\in\mathcal{V}}\left\{\bar{\mathcal{H}}_x^v + \lambda\right\}\tilde{w}_{\lambda,a}(x) = 0 \\ \\ \tilde{w}_{\lambda,\alpha}(x) = F_{\mathcal{I}}(x), \end{cases}$$

if, and only if, the species has a terminal condition, such as maximum age, from (9.15).

14 Semelparous OLSP in a specific model (from partIV)

In our simple model in OLSP, the mature body size and the fertility rate function, $\phi(y)$, should have a unique m for the existence of an optimal life schedule in r-selection. Furthermore, the optimal strategy is favored when mature body size and fertility have the relationship $m \geq \rho_0$ among the life history parameters. Namely, the prosperity of a species requires not only an optimal schedule but also the persistence of the species. The relation of $m \geq \rho_0$ becomes an evaluation criterion of whether the species is persistent.

Life span is an important element of evolution in r-selection. Our simple model shows that the effect of internal stochasticity on fitness and life span is not always negative and increases the number of individuals whose life spans are relatively short. It is the fertility rate function, $\phi(y)$, that determines

whether stochasticity has positive or negative effects on fitness. As a property of the BRN, the more that large stochasticities affect individuals, the more closely the BRN approximates a convergence value (see Fig. 3). Then, the property of $\phi(y)$ gives the BRN its value. In other words, the property of $\phi(y)$ determines whether the reduction of the BRN by stochasticity reaches below 1, as in inequalities (10.13). We show that stochasticity always reduces the age at maturity of individuals because individuals whose maturity is slow are killed by a constant mortality. Since faster maturity is equivalent to a faster alternation of generations, individuals can escape from high mortality ($\mu_0/\gamma > 1$) and save the population from extinction when $\phi(y)$ satisfies the inequality (10.13c), as in Fig. 2. Eventually, once a $\phi(y)$ is given, the optimal body size and the sensitivity of fitness to internal stochasticity are determined because the parameters (γ, σ_0^2, and μ_0) operate fitness monotonically.

From the analysis of this study, internal stochasticity has not only negative but also positive effects on population dynamics. It is therefore not always nonadaptive for a semelparous species to tend to have a short life span in a stochastic environment. This does not contradict empirical results such as those of [2, 3, **?**]. When a species lives in an environment in which

stochasticity has negative effects, individuals may oppose stochasticity, as asserted by Pfister [48]. Note that generally, twofold randomness (internal and external stochasticity) exists in the background of this consideration. Such randomness always affects the fitness λ^* of a TMM as follows:

$$\lambda^* = \bar{\lambda} - \tilde{\sigma}^2/2,$$

where $\bar{\lambda}$ and $\tilde{\sigma}$ represent a maximum eigenvalue of the TMM with no environmental stochasticity and a magnitude of the stochasticity, respectively [4, 5, 6]. However, when a species lives where only internal stochasticity affects its life history, it avails the internal stochasticity to optimize its own life history because it can increase its fitness.

15 Analysis of optimal stochastic growth in a two-resource utilization model (from part V)

The two-resource utilization model shows that optimal strategies behave differently depending on breeding systems and fertility functions, even if a species occurs in the same habitat. Then, the convexity of the objective function is the keyword of all of the optimal strategies analyses in this study. To explain the importance of the convexity, we introduce Jensen's inequality.

Let $f(y)$ be a concave function, such as $f'(y) > 0$ and $f''(y) < 0$. Then, the function satisfies the following inequality for an arbitrary random variable, X_a,

$$\mathbb{E}_x [f(X_a)] \leq f(\mathbb{E}_x [X_a]).$$

Incidentally, as for the convex function, the inequality becomes an opposite magnitude correlation. As Jensen's inequality suggests, the exposure of a species to risk becomes advantageous when the objective function has high convexity. Since the convexity depends on life history, semelparous and iteroparous species possibly have different growth strategies even if they share several elements of life history, such as Eq.(7.1), and $\mu(x, v)$ in the habitat. In this case, the difference in fertility yields different convexities of the objective function and strategies. In other words, the breeding system determines what the species will optimize.

In semelparous species, the parameter m represents an index of the convexity degree in the value function. A positive effect of internal stochasticity is caused by the strength of the index. A trade-off between precocity and prolificacy occurred in the OLSP. Stochasticity yields both precocious and slow-growing individuals. The former cause faster alternations of genera-

tions, while the latter decrease the BRN by increasing the risk of death. The present analysis showed that the index, m, determines the sensitivity of the BRN to stochasticity; especially, a small m decreases the BRN in the domain $m \in (0, 1)$. Consequently, species with small m utilize smaller risk, such as R_2 more than R_1 in the present paper. The optimal utilization, $\tilde{v}_S$, continuously decreases with m. Then, nature selects whether a species is a resource specialist or generalist depending on the index m.

The risk appetite of semelparous species depends on m, composed of the mature body size and $\phi\left(x^*_{opt}\right)$ in the optimal utilization, while that of iteroparous species depends on the allometric exponent β. This has the same characteristic as the index m in the optimal utilization of semelparous species. If a species has a large value of β, the fitness is also high. Those parameters characterize the convexity of the objective function. As Jensen's inequality shows, the convexity determines the effect of internal stochasticity on fitness. A large value of m or β makes the objective function close to a convex function. When they have the same convexity, $m = \beta$, semelparous and iteroparous species have the same risk appetite and the optimal utilization. In contrast, the breeding age distribution of iteroparous species is different

from that of semelparous species. The trend in age distribution depends on $\tilde{\lambda}_{\mathcal{S}}(\beta)$. If $\tilde{\lambda}_{\mathcal{S}}(\beta)$ is positive, the breeding age distribution skews toward older ages (see Eq.(11.28)). Then, the persistence of the species is determined by the maximum age α. Therefore, long-lived individuals are important for population growth in this case.

Another meaning of m and β from a biological point of view is their representation of the conversion efficiency from adult body size to number of offspring. For example, a large value of m means a mature individual producing many offspring and/or having a low ratio of mature body size to initial body size. Therefore, the risk appetite is determined by the conversion efficiency. The evolution of generalists is considered to be related to a portfolio effect in our resource utilization model. The portfolio effect is a species diversifying its resource utilization and diet to reduce risk [49]. This effect has been reported in various cases, such as in salmon [50]. This study shows that the diversification of resource use is important for species susceptible to internal stochasticity (i.e., when m and β are small), which may provide an explanation for the evolution of the portfolio effect.

16 Future work

This study demonstrates that several kinds of optimal growth strategies may exist depending on breeding systems in a simple stochastic growth process. However, the theories presented this study (Eqs.(7.8), (7.9), (9.2), and (9.15)) are also applicable to other events and trade-offs in the life histories of organisms. Moreover, we can extend the one-dimensional theories from this study to an arbitrary dimensional size because the path integral and HJB equations hold an arbitrary dimension.

The controls maximizing the objective function and BRN have basically different meanings. The former simultaneously optimizes the ERS and generation time. In contrast, the latter maximizes only the BRN. Therefore, the optimal control that maximizes the objective function is more complicated a control than the latter. Conversely, Eq.(9.22) shows that both types of controls accord when the mortality does not depend on the control parameter. The analysis of iteroparous species does not need to consider the effects of control on generation time because the model satisfies the condition mentioned above. Considering the mortality controlled, another trade-off occurs between the risk of stochasticity and survivorship. The methods presented

in this study are suitable for use in addressing such subjects and provide a basis for such future research.

Acknowledgments

The author is deeply grateful to Takenori Takada for his helpful comments and advice toward the accomplishment of this study. The author greatly thanks Takashi Kohyama, Toshihiko Hara, Akiko Satake, and Tomonori Sato for their various suggestions. The author also thanks Nobuhiko Fujii, Hisashi Inaba, and Akira Sakai for mathematical advice, and François Feugier, Motohide Seki, Jordan Sinclair, and Jacob Korte for checking and improving this manuscript. The author thanks Hiroko Oizumi (the author's mother), Kumiko Aoki, Yuma Sakai, Yuuki Chino, Kunihiro Aoki, and the SDE reading circle members for supporting and encouraging him. The author thanks his laboratory and Sakai's group members for checking calculations. The author dedicates this thesis with his gratitude to his colleague Shoichi Yamada, who died before achieving his ambition.

Appendix

Appendix A

Derivation of path integral expression

Let (t, a) be fixed and h be a new variable. The LHS of Eq.(2.1) becomes

$$\frac{\partial}{\partial h}\bar{P}_h(y) = \frac{\partial}{\partial t}P_{t+h}(a+h, y) + \frac{\partial}{\partial a}P_{t+h}(a+h, y),$$

and we define

$$\bar{P}_h(y) := P_{t+h}(a+h, y). \tag{A.1}$$

We can then obtain the Fokker–Planck equation with respect to a new population density $\bar{P}_h(y)$ as follows:

$$\begin{cases} \dfrac{\partial}{\partial h}\bar{P}_h(y) = -\mathcal{H}_y\bar{P}_h(y) \\ \bar{P}_0(y) = \bar{n}_0(x)\,\delta(x-y), \end{cases} \tag{A.2}$$

where $\bar{n}_0(x) := n_{t-a}(x)$. To derive the path integral from Eq.(A.2), we use the Fourier transform of the function $\bar{P}_h(y)$ with respect to y, such that

$$\begin{cases} \hat{P}_h(q) := \displaystyle\int_{-\infty}^{\infty} dy \exp\{iqy\}\,\bar{P}_h(y) \\ \hat{P}_0(q) = \bar{n}_0(x)\exp[iqx], \end{cases} \tag{A.3}$$

and substitute it into Eq.(A.2) as follows:

$$\frac{\partial}{\partial h}\hat{P}_h(q) = -\int_{-\infty}^{\infty} dy \exp\{iqy\}\,\mathcal{H}_y\bar{P}_h(y). \tag{A.4}$$

On the right side of the equation, we use integration by parts to obtain

$$\begin{cases} -\int_{-\infty}^{\infty} dy \exp\{iqy\} \mathcal{H}_y \bar{P}_h(y) = -\int_{-\infty}^{\infty} dy \exp\{iqy\} \mathcal{H}_{-iq,y} \bar{P}_h(y) \\ \mathcal{H}_{-iq,y} = -iqg(y) + \frac{1}{2} q^2 \sigma(y)^2 + \mu(y), \end{cases} \tag{A.5}$$

and expand $g(y)$, $\sigma(y)^2$ and $\mu(y)$ into a series, with respect to h as follows:

$$\begin{cases} g(y) = g(x) + \frac{dg(y)}{dy} \frac{dy}{dh}\Big|_{h=0} h + O\left(h^2\right) \\ \sigma(y)^2 = \sigma(x)^2 + \frac{d\sigma(y)^2}{dy} \frac{dy}{dh}\Big|_{h=0} h + O\left(h^2\right) \\ \mu(y) = \mu(x) + \frac{d\mu(y)}{dy} \frac{dy}{dh}\Big|_{h=0} h + O\left(h^2\right). \end{cases} \tag{A.6}$$

Substituting (A.6) into (A.5), we obtain a transition rate for a sufficiently short time, h, which is given by

$$\begin{aligned} \int_{-\infty}^{\infty} dy \exp\{iqy\} \mathcal{H}_y \bar{P}_h(y) &= \left(-\mathcal{H}(-iq, x) + O(h)\right) \hat{P}_h(q) \\ &\approx -\mathcal{H}(-iq, x) \hat{P}_h(q), \end{aligned} \tag{A.7}$$

where

$$\mathcal{H}(-iq, x) = -iqg(x) + \frac{1}{2} q^2 \sigma(x)^2 + \mu(x).$$

Substituting (A.7) into (A.4) and solving the ODE, we obtain the solution

$$\hat{P}_h(q) = n_0(x) \exp\{iqx - \mathcal{H}(-iq, x) h\}.$$

Using the inverse transform of the equation above, $\bar{P}_h(y)$ for a short h becomes

$$\bar{P}_h(y) = \frac{\bar{n}_0(x)}{2\pi} \int_{-\infty}^{\infty} dq \exp\left\{-iq(y-x) - \mathcal{H}(-iq, x)\, h\right\}. \tag{A.8}$$

Setting

$$K_{\Delta h}(x \to y) := \frac{1}{2\pi} \int_{-\infty}^{\infty} dq \exp\left\{-iq(y-x) - \mathcal{H}(-iq, x)\, \Delta h\right\},$$

the dynamics of the Markovian process for the discretized time is expressed by

$$\begin{aligned} K_h(x \to y) &= \int \cdots \int_A \prod_{j=1}^{M-1} dx_j K_{\Delta h}(x_j \to x_{j+1}) \\ &= \frac{1}{(2\pi)^M} \int \cdots \int_A \prod_{j=1}^{M-1} dx_j \int \cdots \int_{-\infty}^{\infty} \prod_{j=0}^{M-1} dq_j \\ &\quad \times \exp\left\{-iq_j(x_{j+1} - x_j) - \mathcal{H}(-iq_j, x_j)\, \Delta h\right\}. \end{aligned} \tag{A.9}$$

Taking the limit of Δh to zero, and keeping $M\Delta h = h$ (a constant),

$$\begin{aligned} &\lim_{\Delta h \to 0} \frac{1}{(2\pi)^M} \int \cdots \int_A \prod_{j=1}^{M-1} dx_j \int \cdots \int_{-\infty}^{\infty} \prod_{j=0}^{M-1} dq_j \\ &\qquad \times \exp\left\{-iq_j(x_{j+1} - x_j) - \mathcal{H}(-iq_j, x_j)\, \Delta h\right\}\Big|_{M\Delta h = h}. \end{aligned} \tag{A.10}$$

Accordingly, the limiting function expresses the summation over every projection function of the sample path that connects x with y at time h and is called the path integral. We rewrite (A.10) as

$$\begin{aligned} K_h(x \to y) &= \int_{X_0=x}^{X_h=y} \mathcal{D}(x) \int_{-\infty}^{\infty} \mathcal{D}(q) \exp\left\{ \int_0^h d\tau \left(-iq_\tau \dot{X}_\tau - \mathcal{H}(-iq_\tau, X_\tau) \right) \right\} \\ \mathcal{H}(-iq_\tau, X_\tau) &:= -iq_\tau g(X_\tau) + q_\tau^2 \sigma(X_\tau)^2 + \mu(X_\tau), \end{aligned} \tag{A.11}$$

where $\dot{X}_\tau$ represents the differential of X_τ with respect to τ, and where

$$\int_{X_0=x}^{X_h=y} \mathcal{D}(x) \int_{-\infty}^{\infty} \mathcal{D}(q) := \lim_{\Delta h \to 0} \frac{1}{(2\pi)^M} \int \cdots \int_A \prod_{j=1}^{M-1} dx_j \int \cdots \int_{-\infty}^{\infty} \prod_{j=0}^{M-1} dq_j.$$

This is the Hamiltonian expression in the path integral. Moreover, calculating the Gauss integral in (A.10) with respect to every q_j, such that

$$\begin{aligned} K_{\Delta h}(x_j \to x_{j+1}) &= \frac{1}{2\pi} \int_{-\infty}^{\infty} dq_j \exp\left\{ -iq_j (x_{j+1} - x_j) - \mathcal{H}(-iq_j, x_j) \Delta h \right\} \\ &= \frac{1}{\sqrt{2\pi\sigma(x_j)^2 \Delta h}} \exp\left\{ -\frac{\left(\frac{x_{j+1}-x_j}{\Delta h} - g(x_j) \right)^2}{2\sigma(x_j)^2} \Delta h - \mu(x_j) \Delta h \right\}, \end{aligned} \tag{A.12}$$

then (A.10) is given by

$$\begin{cases} \lim_{\Delta h \to 0} \int \cdots \int_A \prod_{j=1}^{M-1} \dfrac{dx_j}{\sqrt{2\pi\sigma(x_j)^2 \Delta h}} \prod_{j=0}^{M-1} \exp\{\Delta h \mathcal{L}_j\} \Big|_{M\Delta h = h} \\ \mathcal{L}_j := -\dfrac{\left(\frac{x_{j+1}-x_j}{\Delta h} - g(x_j) \right)^2}{2\sigma(x_j)^2} - \mu(x_j), \end{cases} \tag{A.13}$$

When we set

$$\int_{X_0=x}^{X_h=y} \mathcal{D}(x) := \lim_{\Delta h \to 0} \int \cdots \int_A \prod_{j=1}^{M-1} \frac{dx_j}{\sqrt{2\pi\sigma (x_j)^2 \Delta h}},$$

then, we obtain another expression for the path integral, as follows:

$$\begin{aligned} K_h(x \to y) &= \int_{X_0=x}^{X_h=y} \mathcal{D}(x) \exp\left\{ \int_0^h d\tau \mathcal{L}\left(\dot{X}_\tau, X_\tau\right) \right\} \\ \mathcal{L}\left(\dot{X}_\tau, X_\tau\right) &:= -\frac{\left(\dot{X}_\tau - g(X_\tau)\right)^2}{2\sigma (X_\tau)^2} - \mu(X_\tau), \end{aligned} \tag{A.14}$$

i.e., the Lagrangian expression. For all of these cases, we set $K_0(x \to y) = \delta(x-y)$ Each expression can be derived from the others using the Legendre transform. Considering $t > a$ and reusing the original coordinate, (t, a), in Eqs.(A.11) and (A.14), we obtain

$$P_{t+h}(a+h, y) = n_{t-a}(x) K_{a+h}(x \to y).$$

From this, we have Eq.(3.1) as follows:

$$P_t(a, y) = n_{t-a}(x) K_a(x \to y),$$

where we assume

$$\lim_{a \downarrow 0} K_a(x \to y) := \delta(x-y).$$

Appendix B

Feynman–Kac formula

The Feynman–Kac formula is the most important equation for analyzing the diffusion process in a potential medium. In a sense, the formula represents a differentiation formula, which is extended to a stochastic differential such that

$$d\left(F\left(X_a\right)S\left(a\right)\right) = dF\left(X_a\right)S\left(a\right) + F\left(X_a\right)dS\left(a\right). \tag{B.1}$$

Then, it becomes

$$\begin{aligned} d\left(F\left(X_a\right)S\left(a\right)\right) = &\left[g\left(X_a\right)F'\left(X_a\right) + \frac{\sigma\left(X_a\right)^2}{2}F''\left(X_a\right) - \mu\left(X_a\right)F\left(X_a\right)\right]S\left(a\right)da \\ &+ g\left(X_a\right)F'\left(X_a\right)S\left(a\right)dB_a \end{aligned} \tag{B.2}$$

from a property of the stochastic differential. The Feynman–Kac formula asserts that the expectation of Eq.(B.2) holds if

$$d\mathbb{E}_x\left[F\left(X_a\right)S\left(a\right)\right] = -\bar{\mathcal{H}}_x\mathbb{E}_x\left[F\left(X_a\right)S\left(a\right)\right]da.$$

Therefore, we have

$$\begin{cases} \dfrac{\partial}{\partial a}u_a\left(x\right) = -\bar{\mathcal{H}}_x u_a\left(x\right) \\ \\ u_0\left(x\right) = F\left(x\right). \end{cases}$$

The proof of the formula is in [12, 13].

Derivation of a general $\psi_\lambda(x)$ in a semelparous species

Because X_a has a strong Markov property, that is, is a property of Ito's SDE [12], we can show that

$$\begin{aligned}
\psi_{\mathcal{S}\lambda,x^*}(x) &= \int_0^\infty da \exp\{-\lambda a\} u_a(x) \\
&= \mathbb{E}_x\left[\int_0^\infty da \exp\{-\lambda a\} F_{\mathcal{S}}(X_a) S_{\mathcal{S}}(a)\right] \\
&= \mathbb{E}_x\left[\int_{a^*}^\infty da \exp\{-\lambda a\} F_{\mathcal{S}}(X_a) S_{\mathcal{S}}(a)\right] \leftarrow \text{because of Eq.(6.3)} \\
&= \mathbb{E}_x\left[\exp\{-\lambda a^*\}\int_0^\infty d\tau \exp\{-\lambda\tau\} F_{\mathcal{S}}(X_{\tau+a^*}) S_{\mathcal{S}}(\tau+a^*)\right] \\
&= \mathbb{E}_x\left[\exp\{-\lambda a^*\} S_{\mathcal{S}}(a^*)\int_0^\infty d\tau \exp\{-\lambda\tau\} F_{\mathcal{S}}(X_\tau) S_{\mathcal{S}}(\tau)\right] \\
&= \mathbb{E}_x\left[\exp\{-\lambda a^*\} S_{\mathcal{S}}(a^*)\right]\mathbb{E}_{x^*}\left[\int_0^\infty d\tau \exp\{-\lambda\tau\} F_{\mathcal{S}}(X_\tau) S_{\mathcal{S}}(\tau)\right] \\
&= \mathbb{E}_x\left[\exp\{-\lambda a^*\} S_{\mathcal{S}}(a^*)\right]\phi(x^*). \quad \uparrow \text{using the strong Markov property.}
\end{aligned}$$

Appendix C

Basic optimal strategy theorem

Theorem

Let $\tilde{v}$ *be*

$$\tilde{v} \in \mathcal{V}, \quad \text{s.t.} \quad \lambda^{*,\tilde{v}} = \sup_v \lambda^{*,v},$$

and $\psi_{\lambda}^{v}(x)$ *is given by Eq.*(7.9). *Define* $\tilde{\lambda}$ *by*

$$\tilde{\lambda} := \lambda^{*,\tilde{v}}.$$

Then, we have

$$\psi_{\tilde{\lambda}}^{v}(x) \leq \psi_{\tilde{\lambda}}^{\tilde{v}}(x) \Leftrightarrow \lambda^{*,v} \leq \lambda^{*,\tilde{v}}.$$

Proof. The key point is that $\psi_{\lambda}^{v}(x)$ monotonically decreases in λ and

$$\psi_{\lambda^{*,v}}(x) = 1.$$

Therefore,

$$\psi_{\tilde{\lambda}}^{v}(x) \leq \psi_{\lambda^{*,v}}^{v}(x) = 1 = \psi_{\tilde{\lambda}}^{\tilde{v}}(x),$$

and the result follows trivially. □

Appendix D

The viscosity solution, introduced in the 1980s, is an important concept with regard to Hamiltonian systems [51], and unifies the population vector Hamiltonian and that in control theory.

Definition of viscosity solutions

We set the function

$$H : [0, \alpha) \times A \times \mathbb{R} \times \mathbb{R} \times \mathbb{R}_{+} \mapsto \mathbb{R}.$$

When H is degenerate elliptic in E, it satisfies

$$E_1 \leq E_2 \rightarrow H\left(a, x, p, E_1, w\right) \geq H\left(a, x, p, E_2, w\right),$$

where $a \in [0, \alpha)$, $x \in A$, $p \in \mathbb{R}$, $E \in \mathbb{R}$, and $w \in \mathbb{R}_+$. If the function is a monotonic function in w, it satisfies

$$w_1 \leq w_2 \rightarrow H\left(a, x, p, E, w_1\right) \leq H\left(a, x, p, E, w_2\right).$$

For example, Hamiltonian

$$H_0\left(x, p, E, w\right) = \inf_v \left\{-g\left(x, v\right) p - \frac{1}{2}\sigma\left(x, v\right)^2 E + \left[\mu\left(y, v\right) + \lambda\right] w\right\} - F\left(x\right), \tag{D.1}$$

is a degenerate elliptic, monotonically increasing function. This function is the same Hamiltonian used in the stochastic maximum principle [44]. Then, p, E, and w represent costate variables in the principle. Let H be a degenerate elliptic and monotonic function. A sub-solution in the viscosity sense, $\psi \in C\left(A\right)$, of

$$H\left(x, \frac{\partial}{\partial x}\psi, \frac{\partial^2}{\partial x^2}\psi, \psi\right) = 0 \tag{D.2}$$

is defined by $\psi - \hat{\psi}$ ($\hat{\psi} \in C^2\left(A\right)$) having a maximum value of zero at $\bar{x}$ and $\hat{\psi}$ satisfying

$$H\left(x, \frac{\partial}{\partial x}\hat{\psi}, \frac{\partial^2}{\partial x^2}\hat{\psi}, \hat{\psi}\right)\Big|_{x=\bar{x}} \leq 0. \tag{D.3}$$

A super-solution of Eq.(D.2) in the viscosity sense, $\psi \in C(A)$, is defined by $\psi - \hat{\psi}$ ($\hat{\psi} \in C^2(A)$). It has a minimal value of zero at $\bar{x}$ and $\hat{\psi}$ satisfying

$$H\left(x, \frac{\partial}{\partial x}\hat{\psi}, \frac{\partial^2}{\partial x^2}\hat{\psi}, \hat{\psi}\right)\Big|_{x=\bar{x}} \geq 0. \tag{D.4}$$

When ψ satisfies the sub- and super-solution in the viscosity sense, it is referred to as a "viscosity solution" [47]. Additionally, the viscosity solution of the nonlinear evolutional PDE can be defined as the sub-solution of

$$-\frac{\partial}{\partial a}w + H\left(a, x, \frac{\partial}{\partial x}w, \frac{\partial^2}{\partial x^2}w, w\right) = 0 \tag{D.5}$$

in the viscosity sense. $w \in C([0,\alpha) \times A)$ is defined by $w - \hat{w}$ ($\hat{w} \in C^{1,2}([0,\alpha) \times A)$), having a maximum value of zero at $(\bar{a}, \bar{x})$ and $\hat{w}$ satisfying

$$-\frac{\partial}{\partial a}\hat{w}\Big|_{a=\bar{a},x=\bar{x}} + H\left(a, x, \frac{\partial}{\partial x}\hat{w}, \frac{\partial^2}{\partial x^2}\hat{w}, \hat{w}\right)\Big|_{a=\bar{a},x=\bar{x}} \leq 0. \tag{D.6}$$

A super-solution of Eq.(D.5) in the viscosity sense, $w \in C([0,\alpha) \times A)$, is defined by $w - \hat{w}$ ($\hat{w} \in C^{1,2}([0,\alpha) \times A)$) having a minimum value of zero at $(\bar{a}, \bar{x})$ and $\hat{w}$, satisfying

$$-\frac{\partial}{\partial a}\hat{w}\Big|_{a=\bar{a},x=\bar{x}} + H\left(a, x, \frac{\partial}{\partial x}\hat{w}, \frac{\partial^2}{\partial x^2}\hat{w}, \hat{w}\right)\Big|_{a=\bar{a},x=\bar{x}} \geq 0. \tag{D.7}$$

When w satisfies the sub-solution and the super-solution of the above PDE in the viscosity sense, it is called a"viscosity solution" of the PDE.

The idea of viscosity solutions unifies two analysis techniques: the HJB equation and the maximum principle in control theory [45]. One can then find the correspondence of (p, E, w) to $\left(\frac{\partial}{\partial x}\hat{\psi}, \frac{\partial^2}{\partial x^2}\hat{\psi}, \hat{\psi}\right)$ in Eq.(D.1). The existence of costate variables and the value function are important for optimal control over both the maximum principle and HJB equations. Focusing on the first, second, and third terms of the Hamiltonians in Eqs.(D.1), (7.6), (9.2), and (9.15), they all have a common functional form: $H(x, p, E, w)$, $H\left(x, iq_\tau, (iq_\tau)^2, (iq_\tau)^0\right)$, $H\left(x, \frac{\partial}{\partial x}\tilde{\psi}, \frac{\partial^2}{\partial x^2}\tilde{\psi}, \tilde{\psi}\right)$ and $H\left(x, \frac{\partial}{\partial x}\tilde{w}, \frac{\partial^2}{\partial x^2}\tilde{w}, \tilde{w}\right)$ with respect to each costate variable, respectively. $H\left(x, iq_\tau, (iq_\tau)^2, (iq_\tau)^0\right)$ shows that this Hamiltonian is the conjugate of the Hamiltonian in the path integral, Eq.(7.6), with respect to $-iq_\tau$. Consequently, the fittest has a minimum Hamiltonian in its habitat, and the Hamiltonian naturally appears in our formulation.

Appendix E

Derivation of the nonautonomous path integral expression

Assuming $\tilde{g}$, $\tilde{\sigma}$, and $\tilde{\mu} \in C^{\infty,\infty}$, we consider a nonautonomous age/size-structured PDE

$$\begin{cases} \left[\dfrac{\partial}{\partial t} + \dfrac{\partial}{\partial a}\right] P_t(a,y) = -\mathcal{H}_{a,y} P_t(a,y) \\ \mathcal{H}_{a,y} := \dfrac{\partial}{\partial y}\tilde{g}(a,y) - \dfrac{1}{2}\dfrac{\partial^2}{\partial y^2}\tilde{\sigma}(a,y)^2 + \tilde{\mu}(a,y) \\ P_{t-a}(0,y) = n_{t-a}(x)\,\delta(x-y). \end{cases} \tag{E.1}$$

Let (t,a) be fixed, and h be a new variable. The LHS of Eq.(E.1) becomes

$$\frac{\partial}{\partial h}\bar{P}_h(y) = \frac{\partial}{\partial t}P_{t+h}(a+h,y) + \frac{\partial}{\partial a}P_{t+h}(a+h,y),$$

and we define

$$\begin{aligned} \bar{P}_h(y) &:= P_{t+h}(a+h,y) \\ \bar{g}(h,y) &:= \tilde{g}(a+h,y) \\ \bar{\sigma}(h,y) &:= \tilde{\sigma}(a+h,y) \\ \bar{\mu}(h,y) &:= \tilde{\mu}(a+h,y). \end{aligned} \tag{E.2}$$

The Fokker–Planck equation with respect to the new population density,

$\bar{P}_h(y)$, is given as follows:

$$\begin{cases} \dfrac{\partial}{\partial h}\bar{P}_h(y) = -\mathcal{H}'_{h,y}\bar{P}_h(y) \\ \mathcal{H}'_{h,y} := \dfrac{\partial}{\partial y}\bar{g}(h,y) - \dfrac{1}{2}\dfrac{\partial^2}{\partial y^2}\bar{\sigma}(h,y)^2 + \bar{\mu}(h,y) \\ \bar{P}_0(y) = \bar{n}_0(x)\,\delta(x-y), \end{cases} \tag{E.3}$$

where $\bar{n}_0(x) := n_{t-a}(x)$. To derive the path integral from Eq.(E.3), one uses the Fourier transform of the function $\bar{P}_h(y)$ with respect to y, such that

$$\begin{cases} \hat{P}_h(q) := \displaystyle\int_{-\infty}^{\infty} dy \exp\{iqy\}\,\bar{P}_h(y) \\ \hat{P}_0(q) = \bar{n}_0(x)\exp[iqx], \end{cases} \tag{E.4}$$

When substituted into Eq.(E.3), we have

$$\frac{\partial}{\partial h}\hat{P}_h(q) = -\int_{-\infty}^{\infty} dy \exp\{iqy\}\,\mathcal{H}'_{h,y}\bar{P}_h(y). \tag{E.5}$$

On the RHS, integration by parts is applied, such that

$$\begin{cases} -\displaystyle\int_{-\infty}^{\infty} dy \exp\{iqy\}\,\mathcal{H}'_{h,y}\tilde{P}_h(y) = -\int_{-\infty}^{\infty} dy \exp\{iqy\}\,\mathcal{H}'(h,-iq,y)\,\tilde{P}_h(y) \\ \mathcal{H}'(h,-iq,y) = -iq\bar{g}(h,y) + \dfrac{1}{2}q^2\bar{\sigma}(h,y)^2 + \bar{\mu}(h,y), \end{cases} \tag{E.6}$$

and expand $\bar{g}(h,y)$, $\bar{\sigma}(h,y)^2$, and $\bar{\mu}(h,y)$ into a power series with respect to h as follows:

$$\begin{cases} \bar{g}(h,y) = \bar{g}(0,x) + \dfrac{\partial}{\partial h}\bar{g}(h,y)\Big|_{h=0} h + \dfrac{\partial}{\partial y}\bar{g}(h,y)\dfrac{dy}{dh}\Big|_{h=0} h + O\left(h^2\right) \\ \bar{\sigma}(h,y)^2 = \bar{\sigma}(0,x)^2 + \dfrac{\partial}{\partial h}\bar{\sigma}(h,y)\Big|_{h=0} h + \dfrac{\partial}{\partial y}\bar{\sigma}(h,y)\dfrac{dy}{dh}\Big|_{h=0} h + O\left(h^2\right) \\ \bar{\mu}(h,y) = \bar{\mu}(0,x) + \dfrac{\partial}{\partial h}\bar{\mu}(h,y)\Big|_{h=0} h + \dfrac{\partial}{\partial y}\bar{\mu}(h,y)\dfrac{dy}{dh}\Big|_{h=0} h + O\left(h^2\right). \end{cases} \tag{E.7}$$

Substituting (E.7) into (E.6), we obtain a transition rate for the sufficiently short time, h, given by

$$\int_{-\infty}^{\infty} dy \exp\{iqy\} \mathcal{H}'_{h,y} \bar{P}_h(y) = \left(-\mathcal{H}'(0,-iq,y) + O(h)\right) \hat{P}_h(q)$$
$$\approx -\mathcal{H}'(0,-iq,y) \hat{P}_h(q), \tag{E.8}$$

where

$$\mathcal{H}'(0,-iq,y) = -iq\bar{g}(0,x) + \frac{1}{2}q^2\bar{\sigma}(0,x)^2 + \bar{\mu}(x).$$

Substituting (E.8) into (E.5) and solving the ODE, we obtain the following solution:

$$\hat{P}_h(q) = \bar{n}_0(x) \exp\{iqx - \mathcal{H}'(0,-iq,y)\Delta h\}.$$

Using the inverse transform of the above equation, $\bar{P}_h(y)$ becomes

$$\bar{P}_h(y) = \frac{\bar{n}_0(x)}{2\pi} \int_{-\infty}^{\infty} dq \exp\{-iq(y-x) - \mathcal{H}'(0,-iq,x)h\}. \tag{E.9}$$

Setting

$$\bar{K}_h(x \to y) := \frac{1}{2\pi} \int_{-\infty}^{\infty} dq \exp\{-iq(y-x) - \mathcal{H}'(0,-iq,x)h\},$$

, the dynamics of the Markovian process at discretized time is expressed by

$$\bar{K}_h(x \to y) = \int \cdots \int_A \prod_{j=1}^{M-1} dx_j \bar{K}_{\Delta h}(x_j \to x_{j+1})$$
$$= \frac{1}{(2\pi)^M} \int \cdots \int_A \prod_{j=1}^{M-1} dx_j \int \cdots \int_{-\infty}^{\infty} \prod_{j=0}^{M-1} dq_j$$
$$\times \exp\left\{-iq_j(x_{j+1} - x_j) - \mathcal{H}'(h_j, -iq_j, x_j)\Delta h\right\}, \qquad \text{(E.10)}$$

where $\Delta h := h_{j+1} - h_j \quad (h_{j+1} > h_j > 0)$ and $h_0 = 0$. Taking the limit of Δh to zero and keeping $M\Delta h = h$ (a constant),

$$\lim_{\Delta h \to 0} \frac{1}{(2\pi)^M} \int \cdots \int_A \prod_{j=1}^{M-1} dx_j \int \cdots \int_{-\infty}^{\infty} \prod_{j=0}^{M-1} dq_j$$
$$\times \exp\left\{-iq_j(x_{j+1} - x_j) - \mathcal{H}'(h_j, -iq_j, x_j)\Delta h\right\}\Big|_{M\Delta h = h}. \qquad \text{(E.11)}$$

Accordingly, the limiting function expresses the summation over every projection function of the sample path, which connects x with y at time h; this is the extended path integral. We rewrite (E.11) as

$$\bar{K}_h(x \to y) = \int_{\tilde{X}_0 = x}^{\tilde{X}_h = y} \mathcal{D}(x) \int_{-\infty}^{\infty} \mathcal{D}(q) \exp\left\{\int_0^h d\tau \left(-iq_\tau \dot{\tilde{X}}_\tau - \mathcal{H}'(\tau, -iq_\tau, X_\tau)\right)\right\}$$
$$\mathcal{H}'_{\tau, -iq_\tau, \tilde{X}_\tau} := -iq_\tau \bar{g}\left(\tau, \tilde{X}_\tau\right) + q_\tau^2 \bar{\sigma}\left(\tau, \tilde{X}_\tau\right)^2 + \bar{\mu}\left(\tau, \tilde{X}_\tau\right), \qquad \text{(E.12)}$$

where $\dot{\tilde{X}}_\tau$ represents the differential of $\tilde{X}_\tau$ with respect to τ, and where

$$\int_{\tilde{X}_0 = x}^{\tilde{X}_h = y} \mathcal{D}(x) \int_{-\infty}^{\infty} \mathcal{D}(q) := \lim_{\Delta h \to 0} \frac{1}{(2\pi)^M} \int \cdots \int_A \prod_{j=1}^{M-1} dx_j \int \cdots \int_{-\infty}^{\infty} \prod_{j=0}^{M-1} dq_j.$$

Additionally, calculating the Gauss integral in (E.11) with respect to every q_j, where

$$\begin{aligned} K_{\Delta h}\left(x_j \to x_{j+1}\right) &= \frac{1}{2\pi}\int_{-\infty}^{\infty} dq_j \exp\left\{-iq_j\left(x_{j+1}-x_j\right) - \mathcal{H}'\left(h_j, -iq_j, x_j\right)\Delta h\right\} \\ &= \frac{1}{\sqrt{2\pi\bar{\sigma}\left(h_j, x_j\right)^2 \Delta h}} \exp\left\{-\frac{\left(\frac{x_{j+1}-x_j}{\Delta h} - \bar{g}\left(h_j, x_j\right)\right)^2}{2\bar{\sigma}\left(h_j, x_j\right)^2}\Delta h - \bar{\mu}\left(h_j, x_j\right)\Delta h\right\}, \end{aligned} \tag{E.13}$$

(E.11) is given by

$$\begin{cases} \lim\limits_{\Delta h\to 0}\int\cdots\int_A \prod\limits_{j=1}^{M-1} \dfrac{dx_j}{\sqrt{2\pi\sigma\left(x_j\right)^2\Delta h}} \prod\limits_{j=0}^{M-1} \exp\left\{\Delta h \mathcal{L}'_j\right\}\Big|_{M\Delta h = h} \\ \mathcal{L}'_j := -\dfrac{\left(\frac{x_{j+1}-x_j}{\Delta h} - \bar{g}\left(h_j, x_j\right)\right)^2}{2\bar{\sigma}\left(h_j, x_j\right)^2} - \bar{\mu}\left(h_j, x_j\right), \end{cases} \tag{E.14}$$

When we set

$$\int_{X_0=x}^{X_h=y} \mathcal{D}\left(x\right) := \lim_{\Delta h\to 0}\int\cdots\int_A \prod_{j=1}^{M-1} \frac{dx_j}{\sqrt{2\pi\bar{\sigma}\left(h_j, x_j\right)^2\Delta h}},$$

then, we obtain the Lagrangian expression of the path integral as follows:

$$\begin{aligned} K_h\left(x \to y\right) &= \int_{\tilde{X}_0=x}^{\tilde{X}_h=y} \mathcal{D}\left(x\right) \exp\left\{\int_0^h d\tau \mathcal{L}'\left(\tau, \dot{\tilde{X}}_\tau, \tilde{X}_\tau\right)\right\} \\ \mathcal{L}'\left(\tau, \dot{\tilde{X}}_\tau, \tilde{X}_\tau\right) &:= -\frac{\left(\dot{\tilde{X}}_\tau - \bar{g}\left(\tau, \tilde{X}_\tau\right)\right)^2}{2\bar{\sigma}\left(\tau, \tilde{X}_\tau\right)^2} - \bar{\mu}\left(\tau, \tilde{X}_\tau\right). \end{aligned} \tag{E.15}$$

For all of the cases, we set $K_0\left(x \to y\right) = \delta\left(x-y\right)$ Each expression is derived from the others using the Legendre transform. Considering $t > a$ and reusing

the original coordinate, (t, a), in Eqs.(E.12) and (E.15), we obtain

$$P_{t+h}(a+h, y) = n_{t-a}(x)\,\tilde{K}_{a+h\in(0,\alpha)}(x \to y).$$

Therefore, we have Eq.(9.17) as follows:

$$P_t(a, y) = n_{t-a}(x)\,\tilde{K}_{a\in(0,\alpha)}(x \to y).$$

We assume that

$$\lim_{a\downarrow 0} \tilde{K}_{a\in(0,\alpha)}(x \to y) := \delta(x - y).$$

Appendix F

Analytical solution of population vector in a simple model

The stable population vector $P_t^{\dagger}(a, y)$ is given by

$$P_t^{\dagger}(a, y) = Q_{x,0} \exp\left[\lambda_x^*(t-a)\right] K_a\left(x \to y \middle| y < x^*\right).$$

Then, the fitness is given by Eq.(10.8), and the projection kernel is a solution of the boundary value problem in $K_a(x \to 0) = K_a(x \to x^*) = 0$, and

$$K_a\left(x \to y \middle| y < x^*\right) =$$
$$\frac{1}{\sqrt{2\pi {\sigma_0}^2 a}} \exp\left\{ -\frac{\left[\log\frac{x}{y} - \left(\gamma - \frac{{\sigma_0}^2}{2}\right)a\right]^2}{2{\sigma_0}^2 a} - \mu_0 a \right\}$$
$$- \frac{1}{\sqrt{2\pi {\sigma_0}^2 a}} \exp\left\{ -2\left(\gamma - \frac{{\sigma_0}^2}{2}\right)\frac{\log\frac{x}{y}}{{\sigma_0}^2} - \frac{\left[\log\frac{yx}{x^{*2}} - \left(\gamma - \frac{{\sigma_0}^2}{2}\right)a\right]^2}{2{\sigma_0}^2 a} - \mu_0 a \right\}, \tag{F.1}$$

from the result on p.56 in [15]). $Q_{x,0}$ becomes

$$Q_{x,0} = \frac{\hat{G}_{\lambda_x^*}(x)}{\log\frac{x^*}{x}} \left| \frac{{\sigma_0}^2 \log\phi(x^*)}{\log\frac{x^*}{x}} + \gamma - \frac{{\sigma_0}^2}{2} \right|. \tag{F.2}$$

Appendix G

Derivation of ψ_λ in a simple model

The adjoint operator $\bar{\mathcal{H}}_x$, which is generated by Eq.(10.1) and Eq.(10.2), represents

$$\bar{\mathcal{H}}_x = -\gamma x\frac{d}{dx} - \frac{1}{2}\sigma_0^2 x^2 \frac{d^2}{dx^2} + \mu_0, \tag{G.1}$$

Substituting the operator into Eq.(5.2), we obtain an ODE such that

$$-\gamma x\frac{d}{dx}\psi_{\mathcal{S}\lambda}(x) - \frac{1}{2}\sigma_0^2 x^2 \frac{d^2}{dx^2}\psi_{\mathcal{S}\lambda}(x) + \mu_0\psi_{\mathcal{S}\lambda}(x) + \lambda\psi_{\mathcal{S}\lambda}(x) - F_{\mathcal{S}}(x) = 0, \tag{G.2}$$

where $F_{\mathcal{S}}(x)$ is given by Eq.(6.2) and represents the boundary condition of the ODE (G.2). Because only the condition $x < x^*$ is considered, it is enough to solve the following equation:

$$-\left(\bar{\mathcal{H}}_x + \lambda\right)\psi_{\mathcal{S}\lambda}(x) = 0. \tag{G.3}$$

We then assume a solution $\psi_{\mathcal{S}\lambda}(x) = Cx^{\rho}$ $(C \neq 0)$, and substitute it into (G.3) as follows:

$$\left(\gamma\rho + \frac{1}{2}\sigma_0^2\rho(\rho-1) - \mu_0 - \lambda\right)Cx^{\rho} = 0. \tag{G.4}$$

By solving (G.4) with respect to ρ, we obtain

$$\rho_{\pm} = \frac{1}{2}\left(1 - \frac{2\gamma}{\sigma_0^2}\right) \pm \frac{1}{2}\sqrt{\left(1 - \frac{2\gamma}{\sigma_0^2}\right)^2 + \frac{8\mu_0}{\sigma_0^2} + \frac{8\lambda}{\sigma_0^2}}.$$

From the linearity of (G.3), the solution of the equation can be written as

$$\psi_{\mathcal{S}\lambda}(x) = c_1 x^{\rho_+} + c_2 x^{\rho_-}.$$

Because $\psi_{\mathcal{S}\lambda}(x)$ has to satisfy $\psi_{\mathcal{S}\lambda}(0) = 0$ and $\psi_{\mathcal{S}\lambda}(x^*) = \phi(x^*)$ from $F_{\mathcal{S}}(x)$, we choose $c_1 = \phi(x^*)/x^{*\rho_+}$ and $c_2 = 0$. Therefore, the solution $\psi_{\lambda}(x^*)$ required is given by

$$\psi_{\mathcal{S}_{\lambda,x^*}}(x) = \psi_{\mathcal{S}\lambda}(x) = \phi(x^*)\left(\frac{x}{x^*}\right)^{\rho_\lambda},$$

where

$$\rho_\lambda := \rho_+.$$

Appendix H

Derivation of reproductive success in a simple model

For simplicity, we change the variables in Eq.(5.1) as follows:

$$\begin{cases} z = \log x \\ \\ z^* = \log x^* \\ \\ \exp\left\{-\mu_0 a\right\} w_a\left(z\right) = u_a\left(x\right). \end{cases} \tag{H.1}$$

Then, we obtain

$$\begin{cases} \dfrac{\partial}{\partial a} w_a\left(z\right) = \left(\gamma - \dfrac{{\sigma_0}^2}{2}\right) \nabla_z w_a\left(z\right) + \dfrac{{\sigma_0}^2}{2} \Delta_z w_a\left(z\right) \\ \\ w_0\left(z\right) = F_{\mathcal{S}}\left(\exp\left\{z\right\}\right), \end{cases} \tag{H.2}$$

where ∇_z and Δ_z represent a dimensional nabla and Laplacian, respectively, with respect to z. From Eq.(5.2), $\tilde{\psi}_\lambda\left(z\right)$ is the Laplace transform of $w_a\left(z\right)$, which satisfies

$$\begin{cases} \lambda \tilde{\psi}_\lambda\left(z\right) + \tilde{\mathcal{H}}_z^* \tilde{\psi}_\lambda\left(z\right) = 0 \\ \\ \tilde{\mathcal{H}}_z^* := -\left(\gamma - \dfrac{{\sigma_0}^2}{2}\right) \nabla_z - \dfrac{{\sigma_0}^2}{2} \Delta_z \\ \\ \lim\limits_{z \to -\infty} \tilde{\psi}_\lambda\left(z\right) = 0, \quad \tilde{\psi}_\lambda\left(z^*\right) = \phi\left(\exp\left\{z^*\right\}\right), \end{cases} \tag{H.3}$$

at $z < z*$. Equations (H.2) and (H.3) represent a first passage time problem in Brownian motion, with drift $(\gamma - {\sigma_0}^2/2)$ at $z \to z^*$, (see [13]). The solution

of Eq.(H.3) becomes

$$\tilde{\psi}_{\lambda,z^*}(z) = \phi(\exp\{z^*\}) \exp\{\tilde{\rho}(z - z^*)\}$$

$$\tilde{\rho} = \frac{1}{2}\left(1 - \frac{2\gamma}{{\sigma_0}^2}\right) + \frac{1}{2}\sqrt{\left(1 - \frac{2\gamma}{{\sigma_0}^2}\right)^2 + \frac{8\lambda}{{\sigma_0}^2}}$$

$$= \phi(\exp\{z^*\}) \int_0^\infty da \frac{(z^* - z)}{\sqrt{2\pi {\sigma_0}^2 a^3}} \exp\left\{-\lambda a - \frac{\left[z^* - z - \left(\gamma - \frac{{\sigma_0}^2}{2}\right)a\right]^2}{2{\sigma_0}^2 a}\right\}$$

Therefore, we obtain

$$w_{a,z^*}(z) = \phi(\exp\{z^*\}) \frac{(z^* - z)}{\sqrt{2\pi\sigma_0^2 a^3}} \exp\left\{-\frac{\left[z^* - z - \left(\gamma - \frac{{\sigma_0}^2}{2}\right)a\right]^2}{2{\sigma_0}^2 a}\right\} \quad \text{(H.4)}$$

(see the appendix of [52]). Then, the distribution

$$\mathbb{P}(a \in da) = \frac{(z^* - z)}{\sqrt{2\pi {\sigma_0}^2 a^3}} \exp\left\{-\frac{\left[z^* - z - \left(\gamma - \frac{{\sigma_0}^2}{2}\right)a\right]^2}{2{\sigma_0}^2 a}\right\} da,$$

is an inverse Gaussian distribution [53, 54], and it represents a distribution of the first time passage of Brownian motion at $z \to z^*$. Reusing the original variables in $w_{a,z^*}(z)$, we obtain $u_{a,x^*}(x)$ as follows:

$$u_{\mathcal{S}a}(x) = \phi(x^*) \frac{\log\frac{x^*}{x}}{\sqrt{2\pi {\sigma_0}^2 a^3}} \exp\left\{-\frac{\left[\log\frac{x^*}{x} - \left(\gamma - \frac{{\sigma_0}^2}{2}\right)a\right]^2}{2{\sigma_0}^2 a} - \mu_0 a\right\}. \quad \text{(H.5)}$$

Appendix I

Mature age density of semelparous species in the two-resources utilization model

Because optimal utilization is constant, we can use the mature age distribution, Eq(10.21). The mature age density of a semelparous species follows

$$\begin{aligned}
&\mathbb{A}_{\mathcal{S}}(a) = \\
&= \frac{\log \frac{x^*}{x}}{\sqrt{2\pi\left[\sigma_1^2 v^2 + \sigma_2^2 (1-v)^2\right] a^3}} \\
&\quad \times \exp\left\{ -\frac{\left[\log \frac{x^*}{x} - \left([\gamma_1 (1-v) + \gamma_2 v] - \frac{1}{2}\left[\sigma_1^2 v^2 + \sigma_2^2 (1-v)^2\right]\right) a\right]^2}{2\left[\sigma_1^2 v^2 + \sigma_2^2 (1-v)^2\right] a} + \rho_v \log \frac{x^*}{x} - \mu_0 a \right\} \\
&\rho_v := \frac{1}{2}\left(1 - \frac{2[\gamma_1 (1-v) + \gamma_2 v]}{\sigma_1^2 v^2 + \sigma_2^2 (1-v)^2}\right) \\
&\quad + \frac{1}{2}\sqrt{\left(1 - \frac{2[\gamma_1 (1-v) + \gamma_2 v]}{\sigma_1^2 v^2 + \sigma_2^2 (1-v)^2}\right)^2 + \frac{8\mu_0}{\sigma_1^2 v^2 + \sigma_2^2 (1-v)^2}}.
\end{aligned} \tag{I.1}$$

Reference

References

[1] R. Salguero-Gómez, H. De Kroon, Matrix projection models meet variation in the real world, Journal of Ecology 98 (2) (2010) 250–254.

[2] W. Lauenroth, P. Adler, Demography of perennial grassland plants: survival, life expectancy and life span, Journal of Ecology 96 (5) (2008)

1023–1032.

[3] W. Morris, C. Pfister, S. Tuljapurkar, C. Haridas, C. Boggs, M. Boyce, E. Bruna, D. Church, T. Coulson, D. Doak, et al., Longevity can buffer plant and animal populations against changing climatic variability, Ecology 89 (1) (2008) 19–25.

[4] S. Tuljapurkar, S. Orzack, Population dynamics in variable environments i. long-run growth rates and extinction, Theoretical Population Biology 18 (3) (1980) 314–342.

[5] S. Tuljapurkar, Population dynamics in variable environments. ii. correlated environments, sensitivity analysis and dynamics, Theoretical Population Biology 21 (1) (1982) 114–140.

[6] S. Tuljapurkar, Population dynamics in variable environments. iii. evolutionary dynamics of r-selection, Theoretical Population Biology 21 (1) (1982) 141–165.

[7] H. Caswell, Matrix population models, Wiley Online Library, 2006.

[8] T. Takada, T. Hara, The relationship between the transition matrix model and the diffusion model, Journal of Mathematical Biology 32 (8) (1994) 789–807.

[9] E. Allen, Derivation of stochastic partial differential equations, Stochastic Analysis and Applications 26 (2) (2008) 357–378.

[10] E. Allen, Derivation of stochastic partial differential equations for size- and age-structured populations, Journal of Biological Dynamics 3 (1) (2009) 73–86.

[11] R. Oizumi, T. Takada, Optimal life schedule with stochastic growth in age-size structured models: theory and an application, Journal of Theoretical Biology 323 (2013) 76–89.

[12] B. Øksendal, Stochastic differential equations: an introduction with applications, Springer Verlag, 2003.

[13] I. Karatzas, S. Shreve, Brownian motion and stochastic calculus, Vol. 113, Springer Verlag, 1991.

[14] J. Sinko, W. Streifer, A new model for age-size structure of a population, Ecology (1967) 910–918.

[15] N. Goel, N. Richter-Dyn, et al., Stochastic models in biology., Academic Press., 1974.

[16] R. Feynman, A. Deutsch, C. Eckart, R. Cowen, G. Dieke, A. P. Society, Space-time approach to non-relativistic quantum mechanics, American Physical Society, 1948.

[17] S. Ellner, M. Rees, Integral projection models for species with complex demography, The American Naturalist 167 (3) (2006) 410–428.

[18] S. Ellner, M. Rees, Stochastic stable population growth in integral projection models: theory and application, Journal of mathematical biology 54 (2) (2007) 227–256.

[19] M. Kac, On distributions of certain wiener functionals, Trans. Amer. Math. Soc 65 (1) (1949) 1–13.

[20] M. Suzuki, Passage from an initial unstable state to a final stable state, Adv. Chem. Phys 46 (1981) 195–278.

[21] H. Hara, Path integrals for fokker-planck equation described by generalized random walks, Zeitschrift für Physik B Condensed Matter 45 (2) (1981) 159–166.

[22] C. Chow, M. Buice, Path integral methods for stochastic differential equations, Arxiv preprint arXiv:1009.5966.

[23] R. F. Fox, Functional-calculus approach to stochastic differential equations, Phys. Rev. A 33 (1986) 467–476. doi:10.1103/PhysRevA.33.467. URL http://link.aps.org/doi/10.1103/PhysRevA.33.467

[24] W. Feller, On the integral equation of renewal theory, The Annals of Mathematical Statistics (1941) 243–267.

[25] J. Metz, O. Diekmann, The dynamics of physiologically structured populations, Vol. 68, Springer, 1986.

[26] N. Keyfitz, H. Caswell, Applied mathematical demography, Springer, 2010.

[27] H. Thieme, Mathematics in population biology, Princeton Univ Pr, 2003.

[28] H. Taylor, R. Gourley, C. Lawrence, R. Kaplan, Natural selection of life history attributes: an analytical approach, Theoretical Population Biology 5 (1) (1974) 104–122.

[29] J. Leon, Life histories as adaptive strategies, Journal of theoretical Biology 60 (2) (1976) 301–335.

[30] H. Morimoto, Stochastic control and mathematical modeling, Cambridge Books.

[31] R. MacArthur, E. Wilson, The theory of island biogeography, Princeton Univ Pr, 1967.

[32] E. Pianka, Natural selection of optimal reproductive tactics, American Zoologist 16 (4) (1976) 775–784.

[33] S. Shreve, Stochastic calculus for finance: Continuous-time models, Vol. 2, Springer Verlag, 2004.

[34] F. Black, M. Scholes, The pricing of options and corporate liabilities, The journal of political economy (1973) 637–654.

[35] M. García, F. Picó, J. Ehrlén, Life span correlates with population dynamics in perennial herbaceous plants, American Journal of Botany 95 (2) (2008) 258–262.

[36] G. Letac, V. Seshadri, A characterization of the generalized inverse gaussian distribution by continued fractions, Probability Theory and Related Fields 62 (4) (1983) 485–489.

[37] K. Aase, Optimum portfolio diversification in a general continuous-time model, Stochastic processes and their applications 18 (1) (1984) 81–98.

[38] M. Suzuki, T. Hiura, Allometric differences between current-year shoots and large branches of deciduous broad-leaved tree species, Tree physiology 20 (3) (2000) 203–209.

[39] R. Jensen, P. Lions, P. Souganidis, A uniqueness result for viscosity solutions of second order fully nonlinear partial differential equations, in: Proc. Amer. Math. Soc, Vol. 102, 1988, pp. 975–978.

[40] P. Zuidema, E. Jongejans, P. Chien, H. During, F. Schieving, Integral projection models for trees: a new parameterization method and a validation of model output, Journal of Ecology 98 (2) (2010) 345–355.

[41] D. Cohen, The optimal timing of reproduction, American Naturalist (1976) 801–807.

[42] Y. Iwasa, J. Roughgarden, Shoot/root balance of plants: optimal growth of a system with many vegetative organs, Theoretical Population Biology 25 (1) (1984) 78–105.

[43] S. Peng, A general stochastic maximum principle for optimal control problems, SIAM Journal on control and optimization 28 (1990) 966.

[44] J. Yong, X. Zhou, Stochastic controls: Hamiltonian systems and HJB equations, Vol. 43, Springer Verlag, 1999.

[45] S. Peng, A generalized dynamic programming principle and hamilton-jacobi-bellman equation, Stochastics: An International Journal of Probability and Stochastic Processes 38 (2) (1992) 119–134.

[46] R. Jensen, The maximum principle for viscosity solutions of fully nonlinear second order partial differential equations, Archive for Rational Mechanics and Analysis 101 (1) (1988) 1–27.

[47] M. G. Crandall, H. Ishii, P.-L. Lions, User's guide to viscosity solutions of second order partial differential equations, Bull. Amer. Math. Soc 27 (1) (1992) 1–67.

[48] C. Pfister, Patterns of variance in stage-structured populations: evolutionary predictions and ecological implications, Proceedings of the National Academy of Sciences 95 (1) (1998) 213.

[49] F. Figge, Bio-folio: applying portfolio theory to biodiversity, Biodiversity & Conservation 13 (4) (2004) 827–849.

[50] D. E. Schindler, R. Hilborn, B. Chasco, C. P. Boatright, T. P. Quinn, L. A. Rogers, M. S. Webster, Population diversity and the portfolio effect in an exploited species, Nature 465 (7298) (2010) 609–612.

[51] M. G. Crandall, P.-L. Lions, Viscosity solutions of hamilton-jacobi equations, Trans. Amer. Math. Soc 277 (1) (1983) 1–42.

[52] H. NAKHLE, Partial differential equations: With fourier series and boundary value problems (2005).

[53] M. Tweedie, Statistical properties of inverse gaussian distributions. i, The Annals of Mathematical Statistics 28 (2) (1957) 362–377.

[54] M. Tweedie, Statistical properties of inverse gaussian distributions. ii., The Annals of Mathematical Statistics (1957) 696–705.